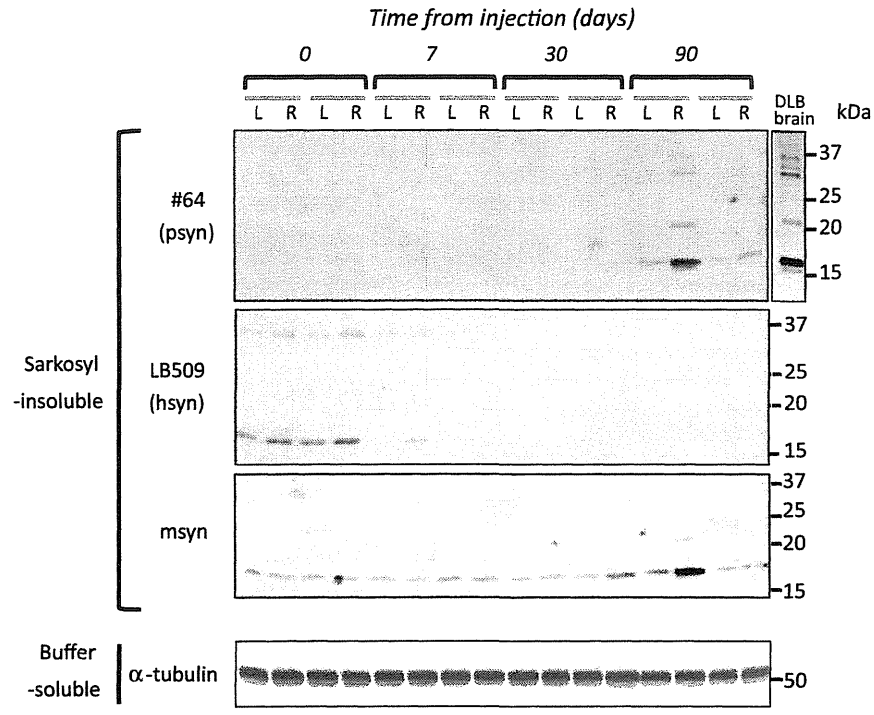

Figure 4 Endogenous mouse α-synuclein was aggregated in wild-type mouse brain injected with human α-synuclein (hsyn) fibrils. The brain was divided into two parts at the longitudinal fissure of the cerebrum. Sarkosyl-insoluble fractions were obtained from the right and left hemispheres, and analysed by immunoblotting with #64, LB509 or anti-mouse α-synuclein (msyn) antibodies. Representative images are shown (n = 14). Sarkosyl-insoluble phosphorylated α-synuclein (psyn) started to accumulate, predominantly in the right hemisphere, at 90 days after injection. It was composed of endogenous mouse α-synuclein, not exogenous human α-synuclein.

dentate gyrus does not have direct projection to substantia nigra, regions connecting with dentate gyrus (i.e., hippocampal CA1, CA3, entorhinal cortex, fimbria, fornix and hippocampal commissure) also showed moderate pathology (Table 1). These results may indicate that α-synuclein pathology propagates unidirectionally through the neural circuit (Supplementary Fig. 8). Spread of pathology from the right hemisphere to the left hemisphere might occur via the corpus callosum, hippocampal commissure, etc., connecting with the contralateral side of the brain (Fig. 3B and Table 1). Phosphorylated α-synuclein pathology in our mouse model was mainly observed in neurons and was hardly detected in glial cells, while the band pattern of sarkosyl-insoluble phosphorylated α-synuclein in mice was indistinguishable from that of dementia with Lewy bodies brains (Fig. 4), where phosphorylated α-synuclein pathology was mainly seen in neurons. Although the mechanism remains to be clarified, exogenous α-synuclein fibrils may enter cells through a selective mechanism(s), such as neuron-specific receptors. Alternatively, differences in expression levels of endogenous α-synuclein or cellular environments may also be important for formation of the pathology, even if abnormal α-synuclein has already entered the cells.

Luk *et al.* (2012*a*) reported dopaminergic neuronal loss and motor dysfunction (by Rotarod test and wire hang test) in wild-type mice injected with mouse α-synuclein fibrils at 6 months after inoculation into striatum. In contrast, our human α-synuclein or mouse α-synuclein fibril-injected mice did not

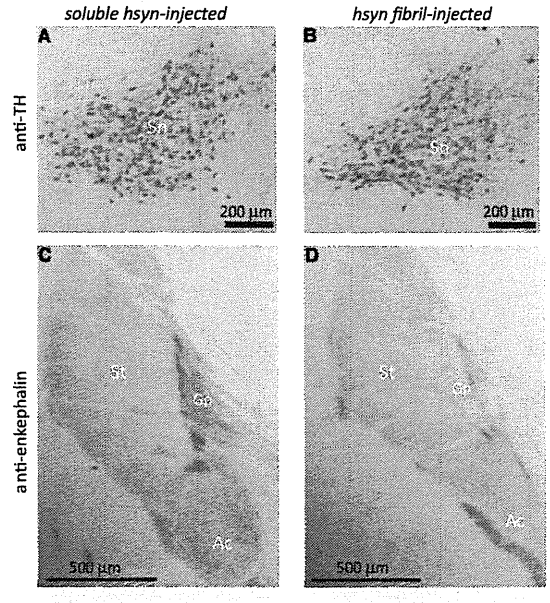

Figure 5 Fibril-injected mice show apparent reduction of a neurotransmitter enkephalin in amygdala central nucleus and globus pallidus at 15 months after injection. Brain sections were stained with anti-tyrosine hydroxylase (TH) (**A** and **B**) and anti-enkephalin (**C** and **D**) antibodies. Ac = amygdala central nucleus; Gp = globus pallidus; Sn = substantia nigra; St = striatum.

Table 2 Comparison of propagation efficiency in mice at 15 months after injection

Injection samples		Right hemisphere (injection side) anti-psyn	anti-ubiquitin	anti-p62	Left hemisphere (non-injected side) anti-psyn
Soluble human α-syn	($n = 8$)	0/8 (0%)	0/8 (0%)	0/8 (0%)	0/8 (0%)
Insoluble human α-syn fibril	($n = 24$)	22/24 (91.6%)	21/24 (87.5%)	22/24 (91.6%)	19/24 (79.2%)
Soluble mouse α-syn	($n = 4$)	0/4 (0%)	0/4 (0%)	0/4 (0%)	0/4 (0%)
Insoluble mouse α-syn fibril	($n = 8$)	8/8 (100%)	7/8 (87.5%)	8/8 (100%)	8/8 (100%)
DLB brain extracts	($n = 14$)	7/14 (50%)	0/14 (0%)	5/14 (35.7%)	1/14 (7.1%)

In the right hemisphere, mice showing immunopositive structures for anti-phosphorylated α-synuclein (psyn), ubiquitin (Ub) or p62 were counted. In the left hemisphere, mice showing immunopositive structures for anti-phosphorylated α-synuclein were counted. Values show number of immunopositive mice/total mice, with percentage of immunopositive mice. DLB = dementia with Lewy bodies.

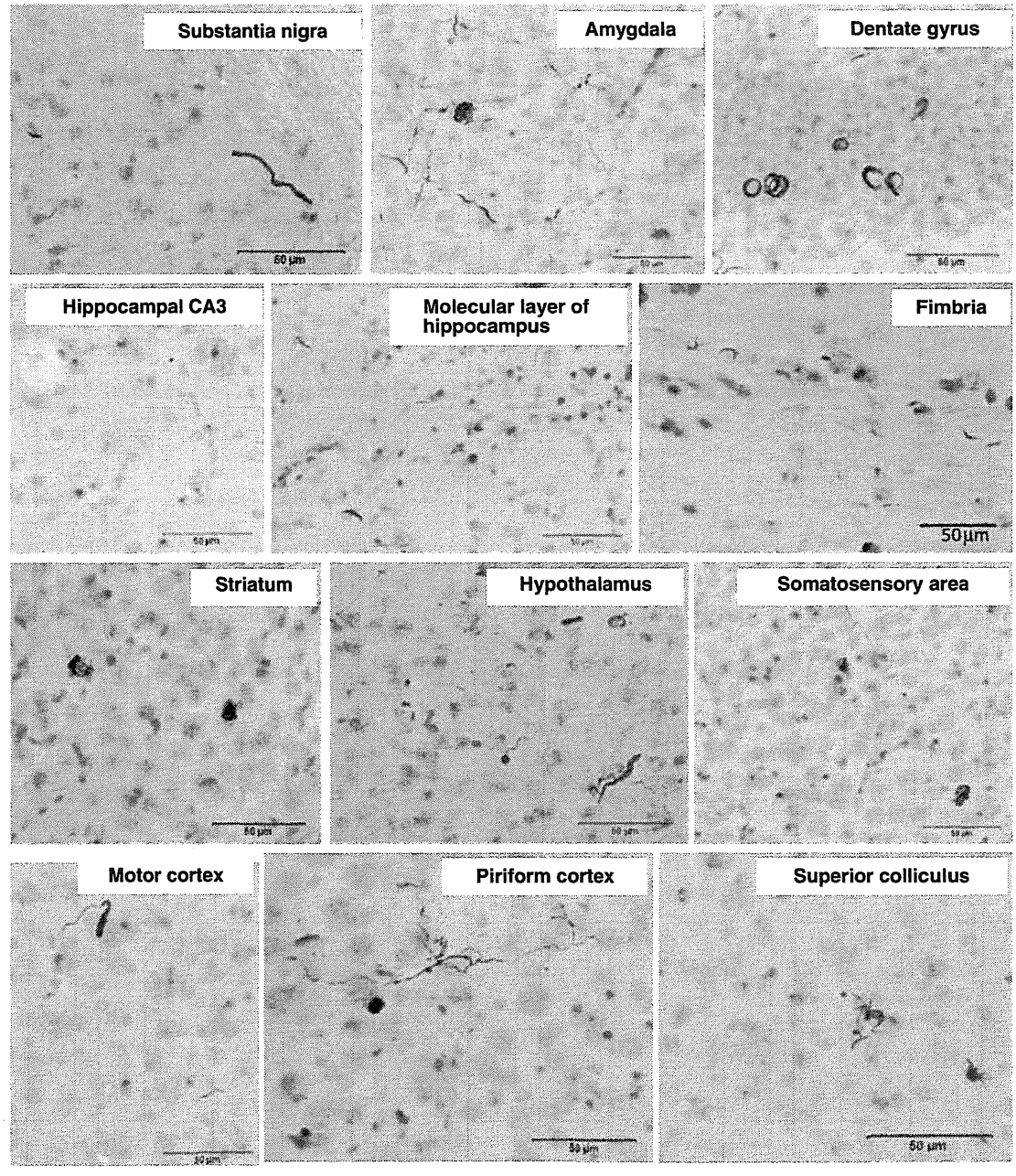

Figure 6 α-Synuclein pathology in wild-type mice brain injected with dementia with Lewy bodies-insoluble fraction observed at 15 months after injection. Sections were immunostained with anti-phosphorylated α-synuclein antibody, 1175.

show any motor and cognitive deficits at 6 months after inoculation and dopaminergic degeneration even after 15 months, a dramatic reduction of enkephalin was observed in the amygdala central nucleus and globus pallidus, with severe pathology, at 6 months after injection (Fig. 5 and Supplementary Fig. 4). The different phenotypes of these mice might be explained by differences in the injection sites [striatum in Luk *et al.* (2012*a*) and substantia nigra in our study]. Nonetheless, the spreading pattern of the pathological α-synuclein is different between our study and theirs. Differential vulnerability of neurons to these abnormal proteins may also affect phenotypes of these mice.

In summary, we have shown that intracerebral injection of insoluble α-synuclein fibrils can induce aggregation of endogenous mouse α-synuclein through a prion-like propagation mechanism. Our data suggest that phosphorylated α-synuclein pathologies do not induce acute neuronal loss but induce a slow neurodegeneration by disrupting neuronal function. These models should be useful not only for elucidating the molecular mechanisms of propagation of intracellular abnormal proteins, but also for development and evaluation of disease-modifying therapy.

Funding

This work was supported by MEXT KAKENHI Grant Numbers 12937622, 12901980 (to M.H.), JSPS KAKENHI Grant Number 11024780 (to M.M-S.) and MHLW Grant Number 12946221 (to M.H.).

Supplementary material

Supplementary material is available at *Brain* online.

References

Baba M, Nakajo S, Tu PH, Tomita T, Nakaya K, Lee VM, et al. Aggregation of alpha-synuclein in Lewy bodies of sporadic Parkinson's disease and dementia with Lewy bodies. Am J Pathol 1998; 152: 879–84.

Braak H, Braak E. Neuropathological stageing of Alzheimer-related changes. Acta Neuropathol 1991; 82: 239–59.

Chartier-Harlin MC, Kachergus J, Roumier C, Mouroux V, Douay X, Lincoln S, et al. Alpha-synuclein locus duplication as a cause of familial Parkinson's disease. Lancet 2004; 364: 1167–9.

Clavaguera F, Bolmont T, Crowther RA, Abramowski D, Frank S, Probst A, et al. Transmission and spreading of tauopathy in transgenic mouse brain. Nat Cell Biol 2009; 11: 909–13.

Desplats P, Lee HJ, Bae EJ, Patrick C, Rockenstein E, Crews L, et al. Inclusion formation and neuronal cell death through neuron-to-neuron transmission of alpha-synuclein. Proc Natl Acad Sci USA 2009; 106: 13010–5.

Emmanouilidou E, Melachroinou K, Roumeliotis T, Garbis SD, Ntzouni M, Margaritis LH, et al. Cell-produced alpha-synuclein is secreted in a calcium-dependent manner by exosomes and impacts neuronal survival. J Neurosci 2010; 30: 6838–51.

Fujiwara H, Hasegawa M, Dohmae N, Kawashima A, Masliah E, Goldberg MS, et al. Alpha-Synuclein is phosphorylated in synucleinopathy lesions. Nat Cell Biol 2002; 4: 160–4.

Goedert M. Alpha-synuclein and neurodegenerative diseases. Nat Rev Neurosci 2001; 2: 492–501.

Ibanez P, Bonnet AM, Debarges B, Lohmann E, Tison F, Pollak P, et al. Causal relation between alpha-synuclein gene duplication and familial Parkinson's disease. Lancet 2004; 364: 1169–71.

Kordower JH, Chu Y, Hauser RA, Freeman TB, Olanow CW. Lewy body-like pathology in long-term embryonic nigral transplants in Parkinson's disease. Nat Med 2008; 14: 504–6.

Kruger R, Kuhn W, Muller T, Woitalla D, Graeber M, Kosel S, et al. Ala30Pro mutation in the gene encoding alpha-synuclein in Parkinson's disease. Nat Genet 1998; 18: 106–8.

Kuusisto E, Salminen A, Alafuzoff I. Ubiquitin-binding protein p62 is present in neuronal and glial inclusions in human tauopathies and synucleinopathies. Neuroreport 2001; 12: 2085–90.

Li JY, Englund E, Holton JL, Soulet D, Hagell P, Lees AJ, et al. Lewy bodies in grafted neurons in subjects with Parkinson's disease suggest host-to-graft disease propagation. Nat Med 2008; 14: 501–3.

Luk KC, Kehm V, Carroll J, Zhang B, O'Brien P, Trojanowski JQ, et al. Pathological alpha-synuclein transmission initiates Parkinson-like neurodegeneration in nontransgenic mice. Science 2012a; 338: 949–53.

Luk KC, Kehm VM, Zhang B, O'Brien P, Trojanowski JQ, Lee VM. Intracerebral inoculation of pathological alpha-synuclein initiates a rapidly progressive neurodegenerative alpha-synucleinopathy in mice. J Exp Med 2012b; 209: 975–86.

Masuda M, Dohmae N, Nonaka T, Oikawa T, Hisanaga S, Goedert M, et al. Cysteine misincorporation in bacterially expressed human alpha-synuclein. FEBS Lett 2006a; 580: 1775–9.

Masuda M, Suzuki N, Taniguchi S, Oikawa T, Nonaka T, Iwatsubo T, et al. Small molecule inhibitors of alpha-synuclein filament assembly. Biochemistry 2006b; 45: 6085–94.

Mougenot AL, Nicot S, Bencsik A, Morignat E, Verchere J, Lakhdar L, et al. Prion-like acceleration of a synucleinopathy in a transgenic mouse model. Neurobiol Aging 2012; 33: 2225–8.

Muller CM, de Vos RA, Maurage CA, Thal DR, Tolnay M, Braak H. Staging of sporadic Parkinson disease-related alpha-synuclein pathology: inter- and intra-rater reliability. J Neuropathol Exp Neurol 2005; 64: 623–8.

Nonaka T, Kametani F, Arai T, Akiyama H, Hasegawa M. Truncation and pathogenic mutations facilitate the formation of intracellular aggregates of TDP-43. Hum Mol Genet 2009; 18: 3353–64.

Nonaka T, Watanabe ST, Iwatsubo T, Hasegawa M. Seeded aggregation and toxicity of {alpha}-synuclein and tau: cellular models of neurodegenerative diseases. J Biol Chem 2010; 285: 34885–98.

Polymeropoulos MH, Lavedan C, Leroy E, Ide SE, Dehejia A, Dutra A, et al. Mutation in the alpha-synuclein gene identified in families with Parkinson's disease. Science 1997; 276: 2045–7.

Prusiner SB. Genetic and infectious prion diseases. Arch Neurol 1993; 50: 1129–53.

Serpell LC, Berriman J, Jakes R, Goedert M, Crowther RA. Fiber diffraction of synthetic alpha-synuclein filaments shows amyloid-like cross-beta conformation. Proc Natl Acad Sci USA 2000; 97: 4897–902.

Shiotsuki H, Yoshimi K, Shimo Y, Funayama M, Takamatsu Y, Ikeda K, et al. A rotarod test for evaluation of motor skill learning. J Neurosci Methods 2010; 189: 180–5.

Singleton AB, Farrer M, Johnson J, Singleton A, Hague S, Kachergus J, et al. alpha-Synuclein locus triplication causes Parkinson's disease. Science 2003; 302: 841.

Spillantini MG, Crowther RA, Jakes R, Hasegawa M, Goedert M. alpha-Synuclein in filamentous inclusions of Lewy bodies from Parkinson's disease and dementia with lewy bodies. Proc Natl Acad Sci USA 1998; 95: 6469–73.

Spillantini MG, Schmidt ML, Lee VM, Trojanowski JQ, Jakes R, Goedert M. Alpha-synuclein in Lewy bodies. Nature 1997; 388: 839–40.

Stohr J, Watts JC, Mensinger ZL, Oehler A, Grillo SK, Dearmond SJ, et al. Purified and synthetic Alzheimer's amyloid beta (Abeta) prions. Proc Natl Acad Sci USA 2012; 109: 11025–30.

Volpicelli-Daley LA, Luk KC, Patel TP, Tanik SA, Riddle DM, Stieber A, et al. Exogenous alpha-synuclein fibrils induce Lewy body pathology leading to synaptic dysfunction and neuron death. Neuron 2011; 72: 57–71.

Wakabayashi K, Yoshimoto M, Tsuji S, Takahashi H. Alpha-synuclein immunoreactivity in glial cytoplasmic inclusions in multiple system atrophy. Neurosci Lett 1998; 249: 180–2.

Yonetani M, Nonaka T, Masuda M, Inukai Y, Oikawa T, Hisanaga S, et al. Conversion of wild-type alpha-synuclein into mutant-type fibrils and its propagation in the presence of A30P mutant. J Biol Chem 2009; 284: 7940–50.

Zarranz JJ, Alegre J, Gomez-Esteban JC, Lezcano E, Ros R, Ampuero I, et al. The new mutation, E46K, of alpha-synuclein causes Parkinson and Lewy body dementia. Ann Neurol 2004; 55: 164–73.

Please cite this article in press as: Nonaka et al., Prion-like Properties of Pathological TDP-43 Aggregates from Diseased Brains, Cell Reports (2013), http://dx.doi.org/10.1016/j.celrep.2013.06.007

Cell Reports
Article

Cell PRESS
Open ACCESS

Prion-like Properties of Pathological TDP-43 Aggregates from Diseased Brains

Takashi Nonaka,[1,*] Masami Masuda-Suzukake,[1] Tetsuaki Arai,[2,3] Yoko Hasegawa,[1] Hiroyasu Akatsu,[4] Tomokazu Obi,[5] Mari Yoshida,[6] Shigeo Murayama,[7] David M.A. Mann,[8] Haruhiko Akiyama,[2] and Masato Hasegawa[1,*]

[1]Department of Neuropathology and Cell Biology
[2]Dementia Research Project
Tokyo Metropolitan Institute of Medical Science, Setagaya-ku, Tokyo 156-8506, Japan
[3]Division of Clinical Medicine, Department of Neuropsychiatry, Faculty of Medicine, University of Tsukuba, Tsukuba, Ibaraki 305-8575, Japan
[4]Choju Medical Institute, Fukushimura Hospital, Toyohashi, Aichi 441-8124, Japan
[5]Shizuoka Institute of Epilepsy and Neurological Disorders, Shizuoka, Shizuoka 420-8688, Japan
[6]Institute for Medical Science of Aging, Aichi Medical University, Nagakute, Aichi 480-1195, Japan
[7]Department of Neuropathology, Tokyo Metropolitan Institute of Gerontology, Itabashi-ku, Tokyo 173-0015, Japan
[8]Centre for Clinical and Cognitive Neuroscience, Institute of Brain Behavior and Mental Health, University of Manchester, Salford M6 8HD, UK
*Correspondence: nonaka-tk@igakuken.or.jp (T.N.), hasegawa-ms@igakuken.or.jp (M.H.)
http://dx.doi.org/10.1016/j.celrep.2013.06.007

SUMMARY

TDP-43 is the major component protein of ubiquitin-positive inclusions in brains of patients with frontotemporal lobar degeneration (FTLD-TDP) or amyotrophic lateral sclerosis (ALS). Here, we report the characterization of prion-like properties of aggregated TDP-43 prepared from diseased brains. When insoluble TDP-43 from ALS or FTLD-TDP brains was introduced as seeds into SH-SY5Y cells expressing TDP-43, phosphorylated and ubiquitinated TDP-43 was aggregated in a self-templating manner. Immunoblot analyses revealed that the C-terminal fragments of insoluble TDP-43 characteristic of each disease type acted as seeds, inducing seed-dependent aggregation of TDP-43 in these cells. The seeding ability of insoluble TDP-43 was unaffected by proteinase treatment but was abrogated by formic acid. One subtype of TDP-43 aggregate was resistant to boiling treatment. The insoluble fraction from cells harboring TDP-43 aggregates could also trigger intracellular TDP-43 aggregation. These results indicate that insoluble TDP-43 has prion-like properties that may play a role in the progression of TDP-43 proteinopathy.

INTRODUCTION

Frontotemporal lobar degeneration (FTLD) and amyotrophic lateral sclerosis (ALS) are well-known neurodegenerative disorders. FTLD is the second most common form of cortical dementia in the population below the age of 65 years (Snowden et al., 2002). ALS is the most common form of motor neuron disease and is characterized by progressive weakness and muscular wasting, and death within a few years. Ubiquitin-positive inclusions composed of misfolded proteins in neuronal and glial cells are common neuropathological features of most neurodegenerative diseases, including Alzheimer's disease (AD), Parkinson's disease (PD), FTLD, and ALS. Recently, TAR DNA-binding protein of 43 kDa (TDP-43) was identified as the major component of inclusions found in the brains of patients with ALS and FTLD (FTLD-U or FTLD-TDP) (Arai et al., 2006; Neumann et al., 2006). TDP-43, a 414-amino-acid protein expressed in nuclei, belongs to the heterogeneous ribonucleoprotein family, members of which are involved in repression of gene transcription, regulation of exon splicing, and nuclear body functions (Buratti and Baralle, 2009; Buratti et al., 2001). TDP-43 is thought to be essential for early embryonic development, because homozygous disruption of the TDP-43 gene (*TARDBP*) causes early embryonic lethality (Sephton et al., 2010; Wu et al., 2010). Interestingly, affected neurons containing cytoplasmic TDP-43 inclusions show depletion of normal nuclear TDP-43 (Arai et al., 2006; Neumann et al., 2006). Patients with these diseases show autosomal-dominant missense mutations in the *TARDBP* gene, mostly located in the C-terminal glycine-rich region (Pesiridis et al., 2009), and pathological TDP-43 is hyperphosphorylated, ubiquitinated, and abnormally cleaved to generate aggregation-prone C-terminal fragments (CTFs) (Arai et al., 2010; Hasegawa et al., 2008, 2011). Thus, loss of normal function of nuclear TDP-43 due to cytoplasmic mislocalization, and toxic gain of function due to cytoplasmic TDP-43 aggregation are potential disease mechanisms (Arai et al., 2006; Neumann et al., 2006).

Aberrant protein aggregates in affected neurons are well-known hallmarks of neurodegenerative diseases, but the mechanisms involved remain unclear. Recent reports suggest that prion-like propagation of protein aggregates composed of tau- or α-synuclein may be involved in progression of neurodegenerative diseases such as AD or PD. This is consistent with findings that tau- or α-synuclein pathology spreads in a

Please cite this article in press as: Nonaka et al., Prion-like Properties of Pathological TDP-43 Aggregates from Diseased Brains, Cell Reports (2013), http://dx.doi.org/10.1016/j.celrep.2013.06.007

Cell PRESS
Open ACCESS

stereotypical temporal and topological manner (Braak and Braak, 1991; Braak et al., 2003). Furthermore, fetal mesencephalic grafts in the striatum of PD patients eventually develop Lewy bodies, suggesting that pathologic α-synuclein could be transmitted from diseased striatal neurons to grafted neurons (Kordower et al., 2008; Li et al., 2008). Cell-cell transmission of tau- and α-synuclein aggregates has been observed in both cell culture and animal models (Clavaguera et al., 2009; de Calignon et al., 2012; Desplats et al., 2009; Frost et al., 2009; Goedert et al., 2010; Liu et al., 2012; Luk et al., 2009, 2012a, 2012b; Nonaka et al., 2010; Masuda-Suzukake et al., 2013). Therefore, prion-like propagation of aberrant protein aggregates may be involved in the pathogenesis of neurodegenerative diseases.

Here, we show that insoluble TDP-43 aggregates in brains of ALS and FTLD-TDP patients have prion-like properties, including the ability to seed intracellular TDP-43 aggregation, stability against heat and proteinases, and cell-to-cell transmissibility.

RESULTS

Intracellular TDP-43 Is Aggregated in a Seed-Dependent Manner

The C-terminal portion of TDP-43 has sequence similarity to prion (Guo et al., 2011). Therefore, to investigate whether intracellular TDP-43 is aggregated in a self-templating manner, like prion, we first established a cell culture model for seeded aggregation of intracellular TDP-43 using SH-SY5Y and 293T cells (Figures 1 and S1A).

We examined whether TDP-43 forms intracellular aggregates in the presence of insoluble TDP-43 prepared from ALS or FTLD-TDP brains as seeds. We observed filamentous structures that were positive for antiphospho TDP-43 (anti-pS409/410) antibody (10–15 nm in diameter) by electron microscopy analyses of insoluble TDP-43 from brains of patients (Figure 1A). Furthermore, it was recently reported that TDP-43 inclusions in ALS and FTLD-TDP showed thioflavin positivity (Bigio et al., 2013). These results clearly indicate that insoluble TDP-43 from brains, used as seeds, had the properties of amyloid. To distinguish plasmid-derived TDP-43 from insoluble TDP-43 introduced as seeds, we used a plasmid encoding hemagglutinin (HA)-tagged TDP-43. SH-SY5Y cells were transiently transfected with HA-tagged TDP-43 and then transduced with or without N-lauroylsarcosine sodium salt (sarkosyl)-insoluble fraction (Sar-ppt) prepared from the brains of ALS (ALS ppt) or FTLD-TDP (FTLD ppt) patients. Cell lysates were fractionated and immunoblotted with anti-HA and anti-pS409/410 antibodies. In cells transfected with HA-TDP-43 plasmid alone, expressed HA-TDP-43 was detected in all fractions with an antibody against HA, whereas phosphorylated HA-TDP-43 was modestly detected in the insoluble fraction (ppt), indicating that the transiently expressed HA-TDP-43 was slightly aggregated (Figure 1B). In cells treated with ALS ppt (5 μg) alone, several bands were detected in ppt fractions with anti-pS409/410, suggesting that endogenous TDP-43 is aggregated in the presence of seeds. On the other hand, in HA-TDP-43-expressing cells transduced with ALS ppt (5 μg), bands with slower mobility were seen with an antibody against HA, and both phosphorylated full-length HA-TDP-43 and its CTFs were detected with anti-pS409/410. We confirmed that plasmid-derived TDP-43, but not ALS ppt seeds, is mainly aggregated in ppt fractions, because no bands were detected with anti-pS409/410 when ALS ppt (5 μg, used as seeds) alone was loaded on the gel (Figure 1C, rightmost lane). Similarly, full-length HA-TDP-43 and CTFs positive for anti-pS409/410 were produced in cells transfected with both HA-TDP-43 plasmid and FTLD ppt (Figures 1B and S1B). Given that plasmid-derived, nontagged TDP-43 was accumulated intracellularly in the presence of ALS ppt (Figure 1C), we mainly used a plasmid encoding, nontagged TDP-43 in subsequent work.

To test whether insoluble TDP-43 in diseased brain extracts can function as seeds for aggregation, we prepared immunodepleted ALS ppt (Figure 1D) as seeds for intracellular TDP-43 aggregation. Sar-ppt of ALS brain was incubated with a mixture of anti-TDP-43 (polyclonal; Proteintech) and anti-pS409/410 antibodies, followed by addition of protein G-Sepharose. After overnight incubation, the supernatant fraction was analyzed by immunoblotting. As shown in Figure 1D (left panel), the immunoreactivity against anti-pS409/410 found in nontreated ALS ppt was wholly lost after immunodepletion (ID). Then, we introduced immunodepleted ALS ppt (ALS ppt ID) into cells expressing HA-TDP-43, using MultiFectam. As shown in Figure 1D (right panel), the band intensities of phosphorylated full-length HA-TDP-43 and CTFs in the ppt fraction of cells expressing HA-TDP-43 and treated with ALS ppt ID were much weaker than those in the case of cells expressing HA-TDP-43 and treated with nonimmunodepleted ALS ppt. We also tested the specificity of ALS ppt as seeds for aggregation of TDP-43. When recombinant α-synuclein fibrils were introduced into cells transiently expressing α-synuclein, phosphorylated α-synuclein was accumulated in Triton-insoluble fractions (Figure S2A), as previously reported (Nonaka et al., 2010). However, intracellular α-synuclein aggregation was not observed in cells expressing α-synuclein and treated with ALS ppt (Figure S2B). Furthermore, HA-TDP-43 was not aggregated in the presence of α-synuclein fibril seeds (Figure S2C). These results showed that insoluble TDP-43 functions specifically as seeds for intracellular aggregation of TDP-43, but not for aggregation of α-synuclein.

We performed immunocytochemical analyses of cells expressing HA-TDP-43 and treated with or without ALS ppt. No phosphorylated and aggregated TDP-43 was seen in cells expressing HA-TDP-43 only (Figure 1E). A few dot-like structures positive for anti-pS409/410 were found in nontransfected cells treated with ALS ppt. On the other hand, round cytoplasmic inclusions of TDP-43 positive for both anti-pS409/410 and an antibody against Ub were detected in cells expressing HA-TDP-43 and treated with ALS ppt. The percentage of HA-positive cells that were also positive for anti-pS409/410 antibody was calculated to be 11.4% ± 4.3%. Interestingly, the immunoreactivity of an antibody against HA in nuclei of cells with cytoplasmic TDP-43 aggregates was less than that in nuclei of cells expressing HA-TDP-43 without aggregates (Figure 1E, lower left), as seen for pathogenic neurons with cytoplasmic TDP-43 inclusions in ALS and FTLD-TDP brains. Taken together, these results suggest that intracellular TDP-43 was efficiently aggregated in cultured cells in a manner that depended on seeding with insoluble TDP-43 derived from patients' brains.

Please cite this article in press as: Nonaka et al., Prion-like Properties of Pathological TDP-43 Aggregates from Diseased Brains, Cell Reports (2013), http://dx.doi.org/10.1016/j.celrep.2013.06.007

Cell PRESS
Open ACCESS

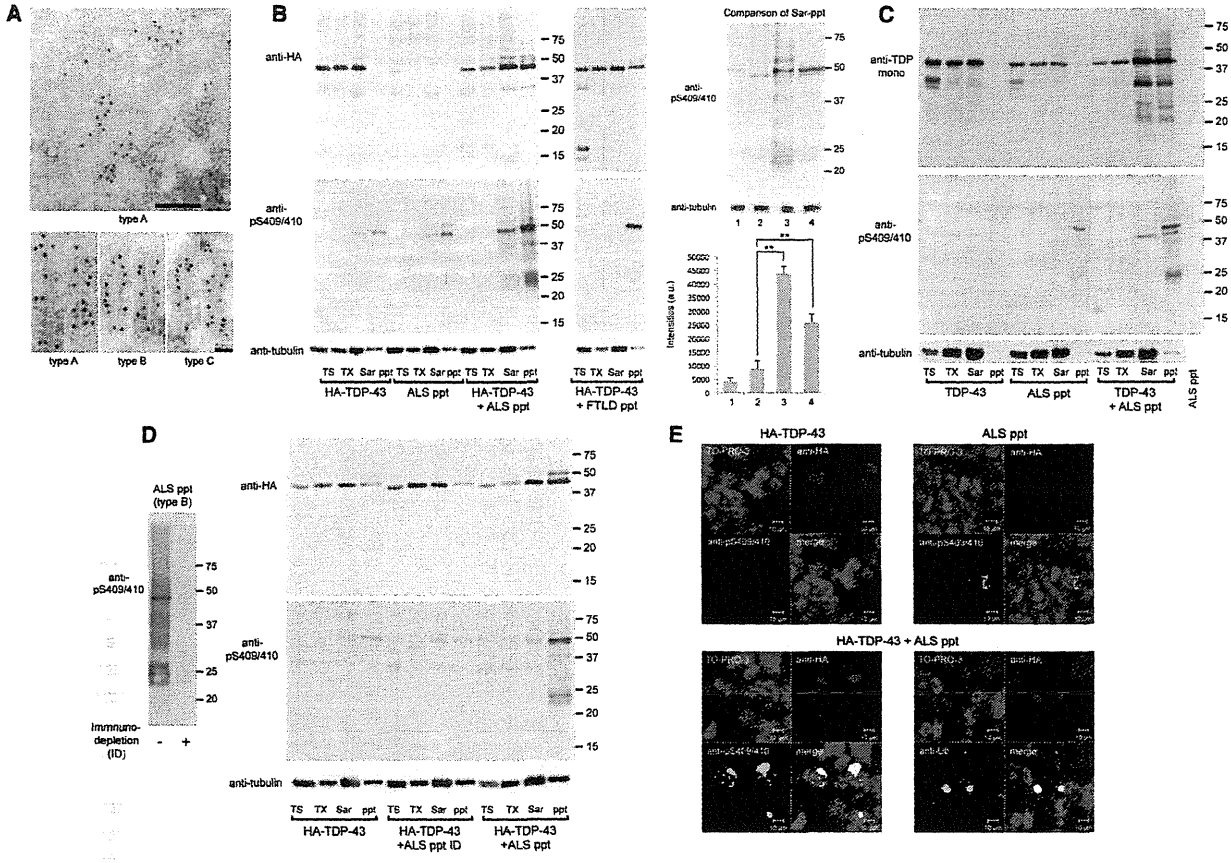

Figure 1. Detergent-Insoluble Fractions from ALS and FTLD-TDP Brains Function as Seeds for Intracellular Aggregation of Plasmid-Derived TDP-43

(A) Immuno-electron microscopy analyses of insoluble fractions from diseased brains (types A, B, and C). Filamentous structures are labeled with anti-phospho TDP-43 antibody (pS409/410). Scale bars represent 200 nm in upper panel, 50 nm in lower panel.

(B) Immunoblot analysis of lysates from cells expressing HA-TDP-43 plasmid only (HA-TDP-43), cells treated with ALS ppt (5 μg; ALS ppt), cells transfected with both HA-TDP-43 and ALS ppt (HA-TDP-43 + ALS ppt), and cells transfected with both HA-TDP-43 and FTLD ppt (5 μg; HA-TDP-43 + FTLD ppt). Proteins were differentially extracted from cells with Tris-HCl (TS), Triton X-100 (TX), and sarkosyl (Sar), leaving the pellet (ppt). Blots were probed using anti-HA (upper) and anti-pS409/410 (lower). In the right panel, the Sar-ppt fractions are shown side by side. 1: HA-TDP-43; 2: ALS ppt; 3: HA-TDP-43 + ALS ppt; 4: HA-TDP-43 + FTLD ppt. The immunoreactivity of each lane that was positive for anti-pS409/410 was quantified and the results are expressed as means + SEM (n = 3). $^{**}p < 0.0005$ by Student's t test; a.u., arbitrary unit.

See also Figure S1.

(C) Immunoblot analysis of proteins extracted from cells expressing only nontagged TDP-43 plasmid (TDP-43), cells treated only with ALS ppt (ALS ppt), and cells transfected with both TDP-43 and ALS ppt (TDP-43 + ALS ppt). Blots were probed using anti-TDP-43 monoclonal antibody (upper) and anti-pS409/410 (lower). No bands were detected when only ALS ppt (5 μg) used as seeds was loaded on the gel (rightmost lane).

(D) ID of ALS ppt was performed with (+) or without (−) a mixture of anti-TDP-43 and anti-pS409/410 antibody. This was followed by immunoblot analyses with anti-pS409/410 (left panel). Proteins differentially extracted from cells expressing only HA-TDP-43 plasmid (HA-TDP-43), and cells transfected with both HA-TDP-43 and immunodepleted ALS ppt (HA-TDP-43 + ALS ppt ID) or untreated ALS ppt (HA-TDP-43 + ALS ppt) were analyzed. Blots were probed using anti-HA (upper) and anti-pS409/410 (lower).

(E) Confocal laser microscopy analyses of cells expressing only HA-TDP-43 plasmid (HA-TDP-43), cells treated with detergent-insoluble fraction of ALS brain (ALS ppt), and cells transfected with both HA-TDP-43 and ALS ppt (HA-TDP-43 + ALS ppt) immunostained with anti-HA (red), anti-pS409/410 (green) or anti-Ub (green), and counterstained with TO-PRO-3 (blue). Scale bars represent 10 μm.

Aggregation of Full-Length TDP-43 Precedes Generation of TDP-43 CTFs

To further investigate the seed-dependent intracellular aggregation of TDP-43, we performed time-course experiments and immunoblot analyses during TDP-43 aggregate formation. Cells expressing HA-TDP-43 and treated with or without ALS ppt were incubated for 1–3 days, and each day the cell lysates were fractionated as described above. No band positive for anti-pS409/410 was detected in any fraction on day 1 or day 2, whereas a weak band of phosphorylated HA-TDP-43 was seen in the insoluble fraction (ppt) on day 3 of cells expressing HA-TDP-43 (Figure 2A). When cells were transfected with both HA-TDP-43

Please cite this article in press as: Nonaka et al., Prion-like Properties of Pathological TDP-43 Aggregates from Diseased Brains, Cell Reports (2013), http://dx.doi.org/10.1016/j.celrep.2013.06.007

Cell PRESS
Open ACCESS

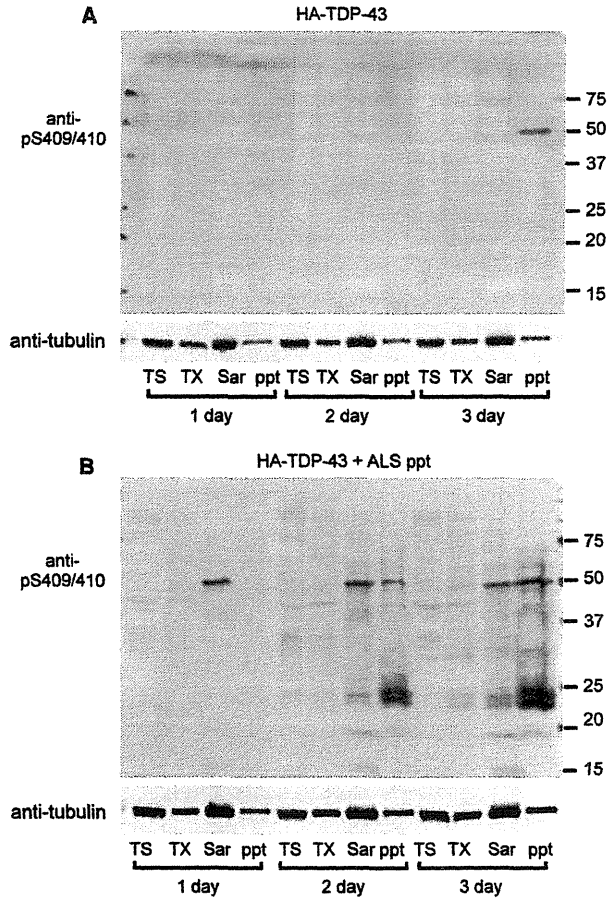

Figure 2. Time Course of Production of TDP-43 CTFs
(A and B) Cells transiently expressing HA-TDP-43 plasmid treated without (A) or with (B) ALS ppt were incubated for 1–3 days and then harvested. Proteins were differentially extracted and subjected to immunoblot analyses. Blots were probed with anti-pS409/410.

plasmid and ALS ppt, surprisingly, full-length HA-TDP-43 was accumulated even on day 1, whereas CTFs were not detected in any fraction at this time (Figure 2B). On and after day 2, not only full-length HA-TDP-43 but also CTFs were aggregated in cells. Thus, intracellular aggregation of full-length TDP-43 precedes generation of TDP-43 CTFs, suggesting that production of CTFs is not essential for formation of intracellular TDP-43 aggregates.

Characteristic CTFs of Insoluble TDP-43 in Each Disease Type Were Reproduced in a Self-Templating Manner in Cultured Cells

TDP-43 proteinopathy is classified into four types based on the predominant TDP-43-positive structures: type A mainly includes FTLD-TDP with GRN mutations, type B contains ALS and FTLD-MND, type C is representative of sporadic FTLD-TDP showing impairment of semantic memory, and type D refers to the pathology associated with inclusion body myopathy with early-onset Paget's disease and frontotemporal dementia caused by *VCP* mutations (Mackenzie et al., 2011). Each type is also characterized biochemically by the patterns of insoluble TDP-43 CTFs detected with anti-pS409/410 (Hasegawa et al., 2008; Tsuji et al., 2012). We prepared Sar-ppt from several types of brains (Figure 3A) and introduced them as seeds into cells expressing a plasmid encoding TDP-43. After 3 days of incubation, cells were harvested and each Sar-ppt was analyzed by immunoblotting with anti-pS409/410. In Figures 3A and 3B, all seeds prepared from TDP-43 proteinopathy brains (Nos. 1–8), but not from DLB (No. 9) or Pick's disease (No. 10) brain, were shown to function as seeds for TDP-43 aggregation in cultured cells, but the seeding efficiencies were different: type A and B seeds were more effective than type C. No sample was available from FTLD-TDP type D brain.

Next, to check whether each characteristic deposit of CTF was reproduced in cultured cells in the presence of each type of seed, we prepared insoluble fractions from TDP-43-expressing cells treated with seeds from each type of brain, and analyzed them by immunoblotting using anti-pS409/410. Interestingly, the band patterns of CTFs in the insoluble fraction (ppt) of cells expressing TDP-43 in the presence of each type of seed were different from each other, but quite similar to that of insoluble TDP-43 prepared as seeds from the corresponding patients (type A, B, or C), indicating that plasmid-derived TDP-43 is aggregated in a template-dependent manner in the presence of each type of seed (Figure 3C). These results suggest that seed-dependent TDP-43 aggregation, like prion aggregation, occurs in a self-templating manner. Insoluble TDP-43 from diseased brains appears to have features similar to those of pathogenic prion.

Insoluble TDP-43 Has Prion-like Properties

Next, we examined whether insoluble TDP-43 from brains of patients has prion-like characteristics. First, we tested whether detergent-insoluble TDP-43 prepared from cells containing TDP-43 aggregates as well as seeds from brains can promote intracellular TDP-43 aggregation. Triton X-100 (TX)-insoluble fraction was prepared as seeds from cells containing aggregates (Figure 4A, right panel) and introduced into cells. In a control experiment, we confirmed that insoluble seeds from cells expressing HA-TDP-43 treated with ALS ppt (HA-TDP-43+ALS ppt) did not serve efficiently as seeds for endogenous TDP-43 aggregation (Figure S3A). In cells expressing HA-TDP-43 and treated with TX-insoluble seeds from cells transfected with both HA-TDP-43 and ALS ppt, phosphorylated full-length HA-TDP-43 and CTFs were observed in the insoluble fraction (ppt; Figure 4A), whereas the band of phosphorylated full-length HA-TDP was hardly detectable in the insoluble fraction from cells expressing HA-TDP-43 and treated with TX-insoluble seed from cells without transfection (none) or treated with TX-insoluble seed from cells expressing HA-TDP-43 alone (HA-TDP-43). In immunocytochemical analyses of cells expressing HA-TDP-43 and treated with TX-insoluble seeds from cells transfected with both HA-TDP-43 and ALS ppt (HA-TDP-43+ALS ppt), we observed inclusions positive for both anti-pS409/410 and anti-Ub (Figure 4B), which were very similar to those observed in cells expressing

Please cite this article in press as: Nonaka et al., Prion-like Properties of Pathological TDP-43 Aggregates from Diseased Brains, Cell Reports (2013), http://dx.doi.org/10.1016/j.celrep.2013.06.007

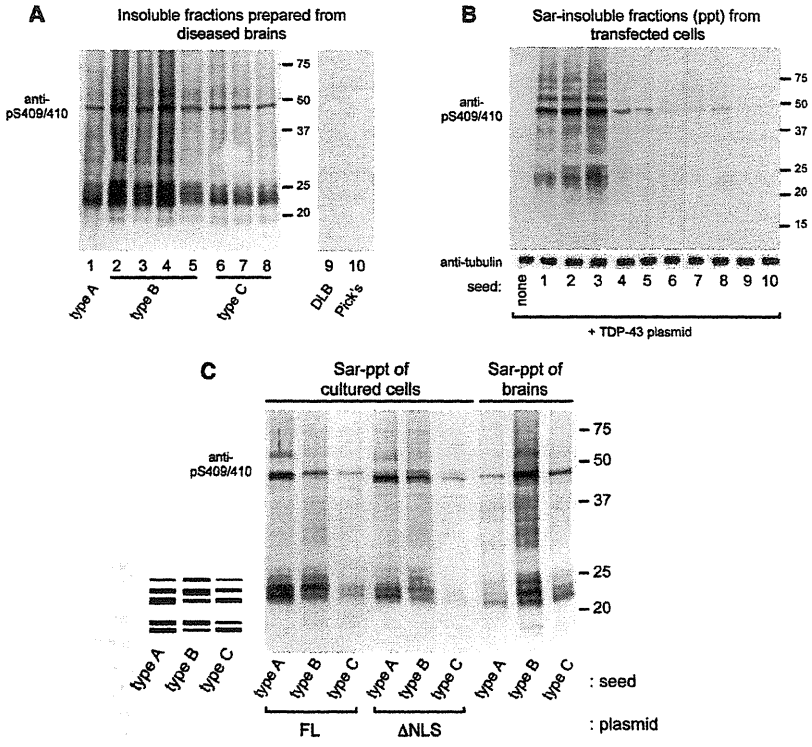

Figure 3. Formation of Self-Templating Aggregates Induced by Insoluble TDP-43 from the Brains of Patients

(A) Immunoblot analyses of Sar-ppt prepared from several diseased brains used as seeds.

(B) Immunoblot analyses of Sar-ppt of cells expressing TDP-43 treated with each seed (Nos. 1–10).

(C) Comparison of band patterns of Sar-ppt fractions from cells expressing full-length TDP-43 (FL) or TDP-43 lacking nuclear localization signal (78–84 residues: ΔNLS) treated with type A, B, or C seed. Sar-ppt fractions from each of the diseased brains are shown next to cellular ppt fractions on the same blot. A schematic diagram of the band pattern of TDP-43 CTFs is also presented. Blots were probed using anti-pS409/410.

HA-TDP-43 treated with ALS ppt (Figure 1E). These results indicate that TX-insoluble seeds produced from cells containing TDP-43 aggregates can function as seeds for further aggregation of TDP-43.

We also checked the effects of heat treatment or proteinase digestion of insoluble TDP-43 on seeding ability. Each type of seed was treated or not treated at 100°C for 5 min (boiling) and analyzed by immunoblotting with anti-pS409/410. No marked differences in the band patterns of each type of seed were seen before or after the boiling treatment (Figure 4C, left panel). Then, these seeds were introduced into TDP-43-expressing cells, and Sar-ppts prepared from the cells were analyzed by immunoblotting with anti-pS409/410 (Figures 4C and S3B). In the case of type A seed, the seeding effect on TDP-43 aggregation was unaffected by boiling, whereas the ability of type B and C seeds to induce TDP-43 aggregation was almost abrogated after boiling (Figure 4C, middle and right panels). All of these seeds were easily degraded into <20 kDa CTFs by Proteinase K (ProK) treatment (Figure 4D, left panel). However, seeding ability to induce intracellular TDP-43 aggregation was retained even after ProK digestion (Figure 4D, middle and right panels, and Figure S3C).

Furthermore, we tested whether formic acid, which destroys the β-sheet structure of proteins, influences the seeding ability of insoluble TDP-43. As shown in Figures 4E, S3D, and S3E, insoluble fractions from type A, B, and C brains treated with formic acid did not induce intracellular TDP-43 aggregation, suggesting that β-sheet-rich structure is necessary for seeding activity. Taken together, these results show that insoluble TDP-43 has prion-like properties, including repeated seeding ability and sensitivity to heat, proteinase, or formic acid.

Intracellular Aggregate Formation of TDP-43 Induces Cell Death in Cultured Cells

To examine whether intracellular TDP-43 aggregates cause neuronal dysfunction leading to cell death, we measured the rate of cell death in cells containing intracellular TDP-43 aggregates by means of lactate dehydrogenase (LDH) assay. Cells transfected with TDP-43 were treated with insoluble fractions from TDP-43 proteinopathy brains or Pick's disease brain and incubated for 3 days, followed by LDH assay. As shown in Figure 5A, the rate of cell death was almost 5% in cells treated only with insoluble fractions from type B or plasmid transfection, whereas it was ~20% in cells expressing TDP-43 and treated with each TDP-43 proteinopathy brain extract. These cell lysates were also analyzed by immunoblotting. Increased cell death of these cells was accompanied by deposition of phosphorylated TDP-43 in the Sar-ppt fraction (Figure 5B). However, no significant cell death was observed in cells expressing TDP-43 and treated with Pick's disease brain extract, in which phosphorylated TDP-43 was not deposited. These results suggest that increased cell death of cells containing TDP-43 aggregates is correlated with the amount of intracellular TDP-43 aggregates.

Intracellular Accumulation of TDP-43 Aggregates Elicits Proteasome Dysfunction

Previously, we reported that proteasome activity was suppressed in cells containing intracellular α-synuclein aggregates (Nonaka et al., 2010). To examine whether intracellular aggregates of TDP-43 also induce proteasome dysfunction, we assayed proteasome activity in cells containing TDP-43 aggregates by using the GFP-CL1 reporter (Bence et al., 2001), which is available to monitor proteasome activity in cultured cells (Nonaka and Hasegawa, 2009; Nonaka et al., 2010).

Please cite this article in press as: Nonaka et al., Prion-like Properties of Pathological TDP-43 Aggregates from Diseased Brains, Cell Reports (2013), http://dx.doi.org/10.1016/j.celrep.2013.06.007

Cell PRESS
Open ACCESS

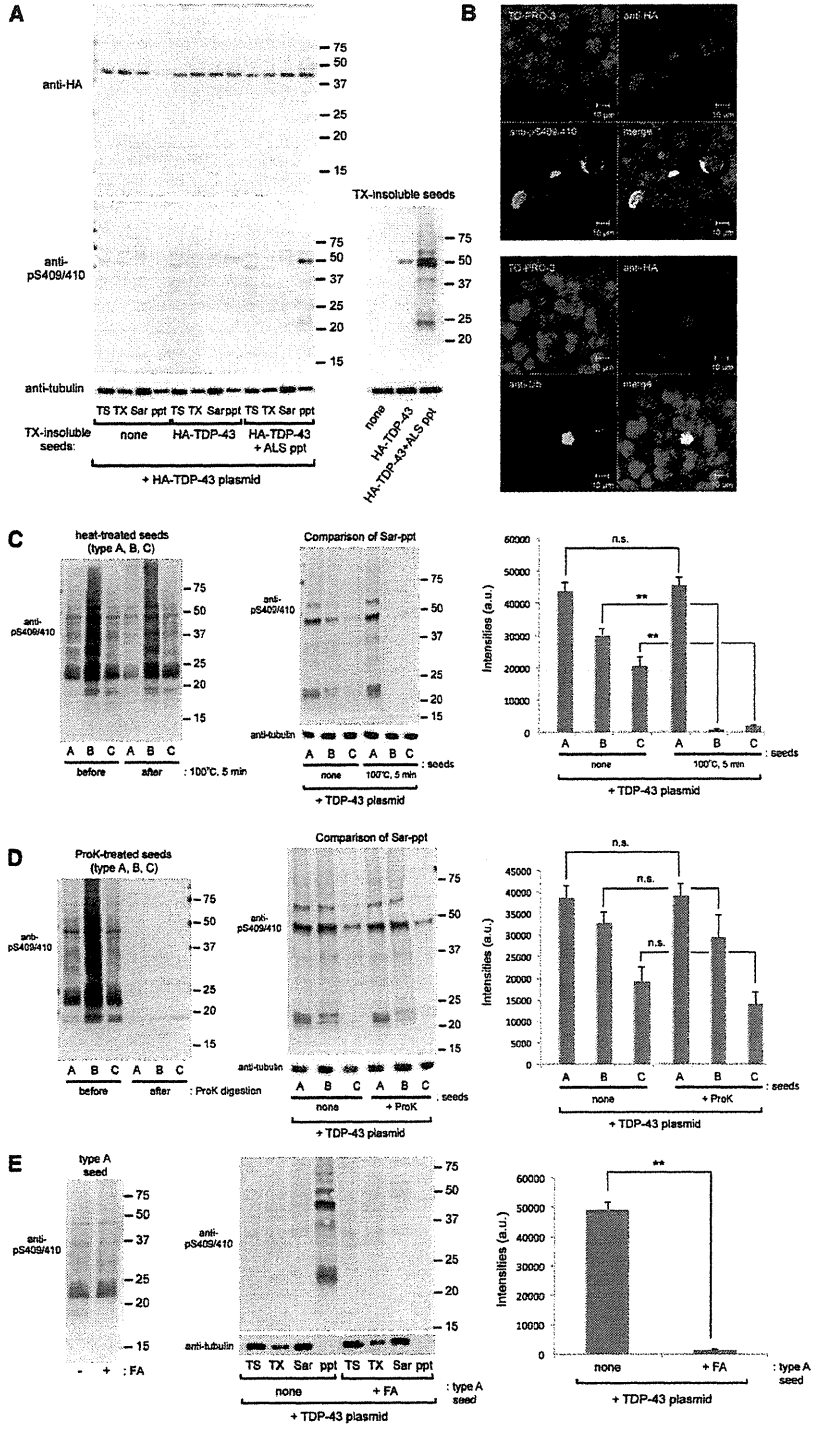

Figure 4. Characterization of the Prion-like Properties of Detergent-Insoluble TDP-43 from Brains

(A) Immunoblot analyses of cells expressing HA-TDP-43 and treated with Triton X-100-insoluble fractions (TX-insoluble seeds) prepared from the following cells, using anti-HA (upper) and anti-pS409/410 (lower): none, mock cells; HA-TDP-43, cells expressing HA-TDP-43; and HA-TDP-43+ALS ppt, cells expressing HA-TDP-43 and treated with ALS ppt. These TX-insoluble seeds (10 μg each) were also immunoblotted with anti-pS409/410 (lower right).

(B) Confocal laser microscopy analyses of cells expressing HA-TDP-43 and treated with TX-insoluble seed from cells transfected with both HA-TDP-43 and ALS ppt (HA-TDP-43+ALS ppt) immunostained with anti-HA (red), anti-pS409/410 (green), or anti-Ub (green), and counterstained with TO-PRO-3 (blue). Scale bars: 10 μm.

(C) Effect of heat treatment on the seeding ability of each type of seed. Each seed before and after heat treatment (100°C for 5 min) was analyzed by immunoblotting using anti-pS409/410 (left). Then, cells expressing TDP-43 were treated with these fractions as seeds. After 3 days of incubation, Sar-ppt fractions were prepared and analyzed by immunoblotting using anti-pS409/410 (middle). The immunoreactivity of each lane that was positive for anti-pS409/410 was quantified and the results are expressed as means + SEM (n = 3). **p < 0.0001 by Student's t test; n.s., not significant; a.u., arbitrary unit. See also Figure S3.

(D) Effect of ProK on the seeding ability of each type of seed. Each seed before and after ProK digestion (final 20 μg/mL ProK at 37°C for 30 min) was analyzed by immunoblotting using anti-pS409/410 (left). Then, cells expressing TDP-43 were treated with these fractions as seeds. After 3 days of incubation, the Sar-ppt fractions were analyzed by immunoblotting using anti-pS409/410 (middle). The immunoreactivity of each lane that was positive for anti-pS409/410 was quantified and the results are expressed as means + SEM (n = 3). n.s., not significant; a.u., arbitrary unit. See also Figure S3.

(E) Effect of formic acid (FA) on the seeding ability of type A seed. Type A seed with or without FA treatment was analyzed by immunoblotting using anti-pS409/410 (left). Then, cells expressing TDP-43 were treated with these fractions as seeds. After 3 days of incubation, fractionated samples were analyzed by immunoblotting using anti-pS409/410 (right). The immunoreactivity of ppt fractions that were positive for anti-pS409/410 was quantified and the results are expressed as means + SEM (n = 3). **p < 0.0001 by Student's t test. a.u., arbitrary unit. See also Figure S3.

Cells were transfected with TDP-43 and GFP-CL1 plasmids overnight, followed by transduction of ALS ppt. After 3 days of incubation, the cells were analyzed by confocal microscopy and immunoblotting. As shown in Figures 6A and 6B, GFP fluorescence in cells transfected with GFP-CL1 alone was very low due to degradation of GFP-CL1 by proteasome. When cells expressing GFP-CL1 were treated with proteasome inhibitor MG132 (0.1 μM), GFP fluorescence intensity

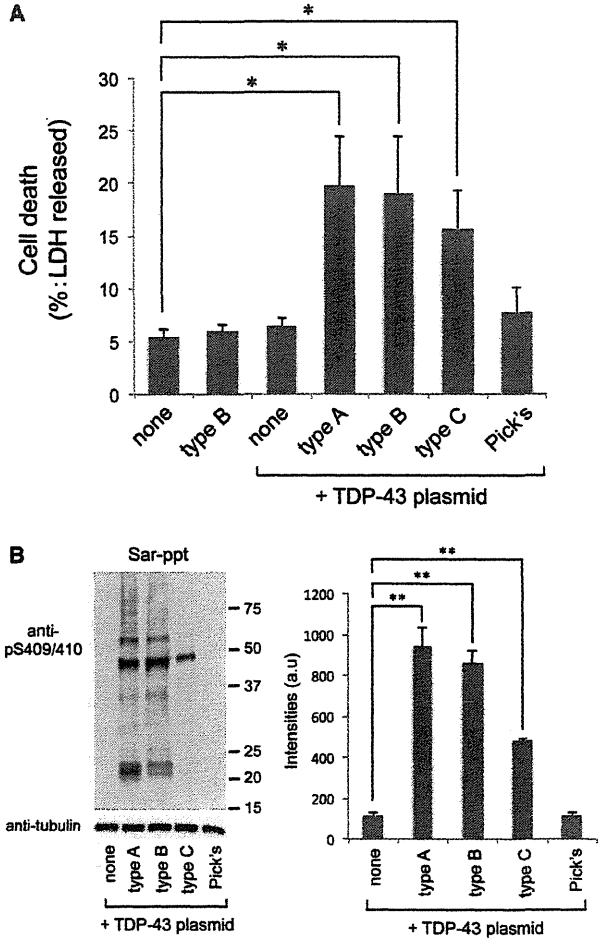

Figure 5. Cell Death Induced by the Formation of Intracellular TDP-43 Aggregates

(A) The extent of cell death of transfected cells was quantified by an LDH release assay. Cells treated with type B seed alone (type B), cells transfected with TDP-43 plasmid alone, or cells expressing TDP-43 and treated with Sar-ppt from type A, B, or C, or Pick's disease brains were cultured, and a cell death assay was performed 3 days thereafter. The results are expressed as means + SEM (n = 5). *$p < 0.05$ versus "none" by Student's t test.

(B) Immunoblot analyses of Sar-ppt from cells expressing TDP-43 and treated with extracts of type A, B, C, and Pick's disease brains, using anti-pS409/410. Immunoreactivity to anti-pS409/410 was quantified in each lane. The results are expressed as means + SEM (n = 3). **$p < 0.001$ versus "none" by Student's t test. a.u., arbitrary unit.

was significantly higher. GFP fluorescence in cells transfected with TDP-43 alone or treated with ALS ppt alone was as low as that in cells expressing only GFP-CL1, whereas it was significantly higher in cells expressing TDP-43 and treated with ALS ppt. We confirmed that cells containing phosphorylated TDP-43 aggregates were strongly positive for GFP (Figure 6C). These results suggest that proteasome activity is suppressed in cells harboring intracellular TDP-43 aggregates.

Phosphorylated TDP-43 Aggregates Are Propagated between Cultured Cells

To examine whether TDP-43 aggregates can be transferred between cultured cells, we performed coculture experiments. SH-SY5Y cells expressing only DsRed were cocultured with SH-S5Y5 cells harboring phosphorylated TDP-43 aggregates in a 1:1 ratio. After incubation for 3 days, the cells were stained with anti-pS409/410 and analyzed by confocal laser microscopy. The presence of phosphorylated TDP-43 aggregates immunolabeled with Alexa-488 in cells expressing DsRed would indicate that phosphorylated TDP-43 aggregates could spread to cells that originally did not contain these aggregates. As shown in Figures 7A and 7B, phosphorylated TDP-43 aggregates (green) were found in the cytoplasm of cells expressing DsRed. The percentage of DsRed-positive cells that also contained phosphorylated TDP-43 aggregates was calculated to be 2.9% ± 0.8%. In three-dimensional image modeling of a DsRed-expressing cell with TDP-43 aggregates, the signal of phosphorylated TDP-43 aggregates was merged with that of DsRed in the X-Z and Y-Z cross-sections (Figure 7B).

Next, we examined how TDP-43 aggregates are released from cells. It has been hypothesized that protein aggregates are released via exosome (Fevrier et al., 2004; Goedert et al., 2010). To investigate whether this mechanism operates for TDP-43 aggregates, we prepared exosome fractions from cells expressing TDP-43 plasmid alone, cells treated with ALS ppt alone, or cells expressing TDP-43 and treated with ALS ppt using the ExoQuick-TC kit (SBI). Immunoblot analyses showed that in cells expressing TDP-43 and treated with ALS ppt, the band intensity of full-length TDP-43 in the exosome fraction was significantly increased as compared with that in cells transfected with TDP-43 plasmid or ALS ppt alone (Figure 7C), whereas expression of the exosome marker protein CD63 was similar in all of the exosome fractions. These results suggest the possibility that exosome may contribute to the release of intracellular TDP-43 aggregates.

DISCUSSION

Prion-like propagation of aggregated proteins in neurodegenerative diseases is well established (Clavaguera et al., 2009; Desplats et al., 2009; Frost et al., 2009; Goedert et al., 2010; Kordower et al., 2008; Li et al., 2008; Luk et al., 2009; Nonaka et al., 2010; Masuda-Suzukake et al., 2013; Polymenidou and Cleveland, 2011; Ren et al., 2009). Here, we show that insoluble TDP-43 prepared from TDP-43 proteinopathy brains (type A, B, and C) can function as seeds for intracellular TDP-43 aggregation in cultured cells. Type A, B, and C brains showed distinct banding patterns of TDP-43 CTFs in immunoblot analyses with anti-pS409/410 (Hasegawa et al., 2008; Tsuji et al., 2012). The band patterns of characteristic CTFs are thought to reflect structural differences of TDP-43 fibrils deposited in each type of brain (Hasegawa et al., 2008; Tsuji et al., 2012). Interestingly, band patterns of CTFs characteristic of the individual seeds were seen in intracellular TDP-43 aggregates in cultured cells, indicating that plasmid-derived TDP-43 aggregation occurs in a self-templating manner. The seeding activity of insoluble TDP-43 from patients' brains was stable against detergents, heat

Please cite this article in press as: Nonaka et al., Prion-like Properties of Pathological TDP-43 Aggregates from Diseased Brains, Cell Reports (2013), http://dx.doi.org/10.1016/j.celrep.2013.06.007

Cell PRESS
Open ACCESS

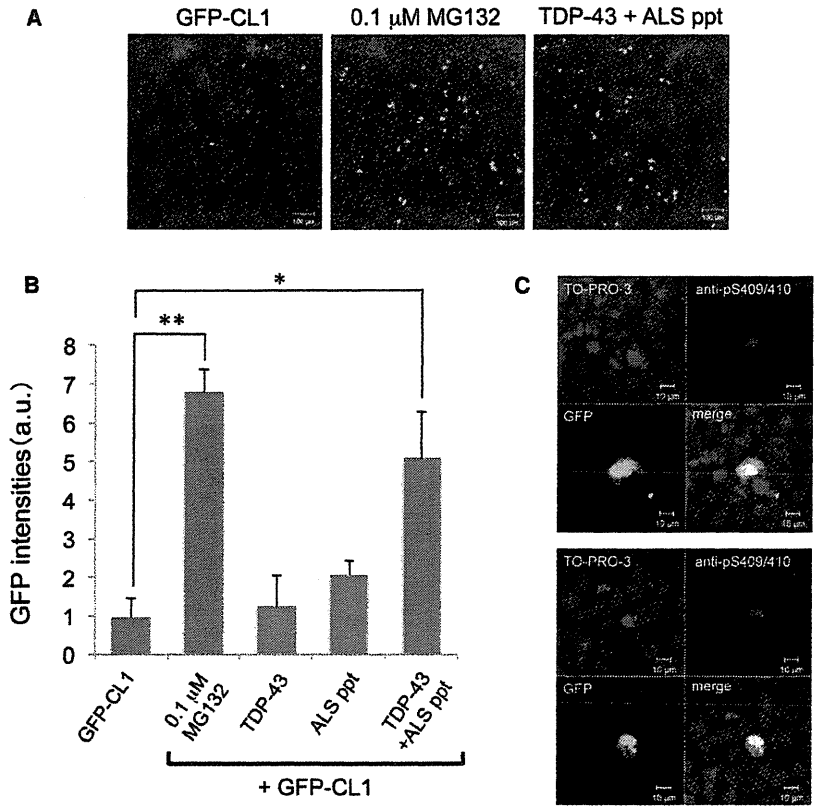

Figure 6. Proteasome Dysfunction in Cells Bearing Intracellular TDP-43 Aggregates

(A–C) SH-SY5Y cells transfected with both GFP-CL1 and TDP-43 were treated with ALS ppt for 2 days.

(A) As a control, cells expressing GFP-CL1 with or without 0.1 μM MG132 or ALS ppt, and cells expressing both GFP-CL1 and TDP-43 were also analyzed.

(B) The intensity of GFP fluorescence in these cells was quantified. The results are expressed as means + SEM (n = 3). *$p < 0.05$; **$p < 0.001$ versus the value of GFP-CL1 by Student's t test. a.u., arbitrary unit.

(C) Cells transfected with both GFP-CL1 and TDP-43 and treated with ALS ppt were stained with anti-pS409/410.

treatment, or proteolytic digestion, and cell-to-cell transmission ability was retained. Formic acid abrogated the seeding ability, suggesting that β-sheet structure in insoluble TDP-43 is indispensable for this ability. Thus, insoluble TDP-43 in the brains of patients has the characteristics of a pathogenic prion, suggesting that TDP-43 proteinopathy involves mechanisms similar to those of prion disease. It remains unclear, however, how protein aggregates spread between cells in vivo. It seems likely that prion-like aggregates are released from cells and taken up by neighboring cells, where they penetrate the cytoplasm and act as nuclei for further aggregation (Goedert et al., 2010). Prions are transferred between cultured cells via exosomes or tunneling nanotubes (Fevrier et al., 2004; Gousset et al., 2009), and our results indicate that TDP-43 aggregates may also be transferred from cell to cell at least partly via exosomes. Further investigation is needed to elucidate in detail the mechanisms of intercellular propagation of protein aggregates in vitro and in vivo. Nevertheless, taken together, our data suggest that TDP-43 proteinopathy can be classified as a prion disease.

Phosphorylated TDP-43 CTFs, as well as phosphorylated full-length TDP-43, are deposited in affected neurons in TDP-43 proteinopathy (Hasegawa et al., 2008, 2011). TDP-43 CTFs identified in FTLD-TDP brains are more prone to form aggregates than the full-length molecule in cultured cells (Igaz et al., 2009; Nonaka et al., 2009). Further, they bind with full-length TDP-43 and may facilitate aggregation of full-length TDP-43 in cultured cells (Budini et al., 2012; Nonaka et al., 2009; Zhang et al., 2009). Therefore, generation of pathogenic TDP-43 CTFs may be crucial for the formation of intracellular TDP-43 inclusions leading to neuronal cell death. However, our time-course immunoblotting analyses (Figure 2) showed that full-length TDP-43 aggregation preceded the deposition of CTFs, suggesting that cleavage of TDP-43 to produce CTFs is not a trigger for intracellular TDP-43 aggregate formation. Thus, it appears that the generation of CTFs is a consequence of degradation of phosphorylated full-length TDP-43 to eliminate abnormal and toxic aggregates of TDP-43, rather than a cause of aggregation of full-length TDP-43. In other words, TDP-43 CTFs deposited in affected neurons represent the residual stable core portion of TDP-43 aggregates left after degradation by intracellular proteolytic systems.

Abnormal posttranslational modifications and abnormal structure of seeds for aggregation are important for reproducing the pathological and biochemical features of TDP-43 inclusions found in the brains of patients with TDP-43 proteinopathy in cultured cells. Indeed, intracellular TDP-43 aggregates obtained using recombinant TDP-43 fibrils as seeds appeared as very small dot-like structures without phosphorylation (Furukawa et al., 2011), and were quite different from the TDP-43 inclusions found in the brains of patients. Our model for seeded aggregation of TDP-43 seems consistent with the pathological and biochemical changes found in the brains of patients with TDP-43 proteinopathy: in the model, aggregated TDP-43 is phosphorylated and ubiquitinated, and immunoreactivity of TDP-43 in nuclei of cells containing cytoplasmic TDP-43 aggregates is relatively weak. We also observed significant cell death and proteasome dysfunction associated with the presence of intracellular TDP-43 aggregates. It is possible that such proteasome dysfunction is caused by overloading of the ubiquitin-proteasome system with ubiquitinated proteins, including TDP-43 aggregates. The resulting suppression of proteasome activity might induce cell death. We previously observed a similar phenomenon (Nonaka et al., 2010); i.e., seed-dependent intracellular

Please cite this article in press as: Nonaka et al., Prion-like Properties of Pathological TDP-43 Aggregates from Diseased Brains, Cell Reports (2013), http://dx.doi.org/10.1016/j.celrep.2013.06.007

Cell PRESS
Open ACCESS

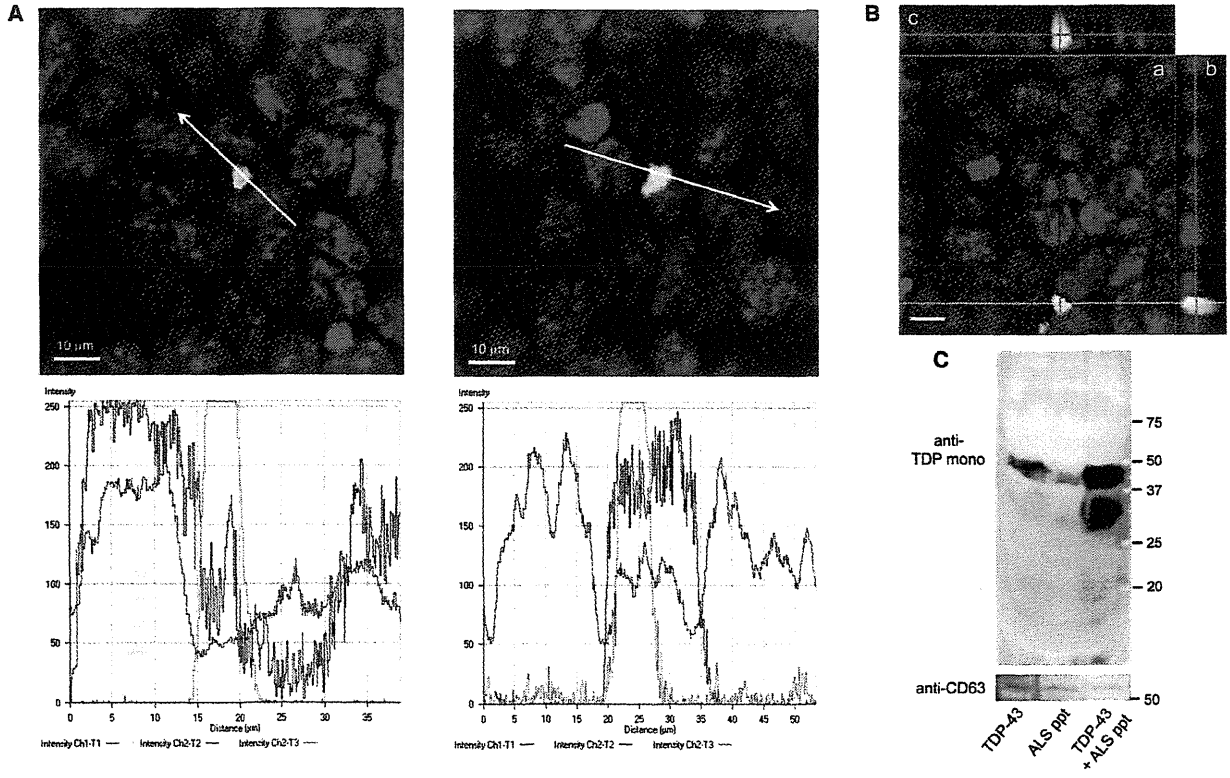

Figure 7. Intracellular TDP-43 Aggregates Are Released in Association with Exosome

(A) Coculture of cells expressing DsRed and cells having intracellular TDP-43 aggregates in a 1:1 ratio. After incubation for 3 days, cells were stained with pS409/410 (green) and counterstained with TO-PRO-3 (blue). The graphs show the intensity distribution profile of DsRed (red line), phosphorylated TDP-43 (green line), and TO-PRO-3, a nuclear marker (blue line), in the merged image. Scale bars: 10 μm.

(B) Cross-sections of reconstructed TDP-43 aggregates in these cocultured cells. (a) One of the optical sections (X-Y) at the depth indicated with blue lines in (b) and (c). (b) Cross-sectional Y-Z image along the green line indicated in (a). (c) Cross-sectional X-Z image along the red line indicated in (a). Red, DsRed; green, phosphorylated TDP-43 aggregate positive for anti-pS409/410; blue, TO-PRO-3 (nuclei). Scale bars: 10 μm.

(C) Immunoblot analyses of exosome fractions prepared from culture medium of cells expressing TDP-43 (TDP-43), cells treated with ALS ppt alone (ALS ppt), and cells expressing TDP-43 and treated with ALS ppt (TDP-43+ALS ppt). Blots were probed with anti-TDP-43 monoclonal (ProteinTech) and an antibody against CD63 (SBI).

aggregation of α-synuclein caused proteasome dysfunction and cell death.

In summary, our results show that insoluble TDP-43 in the brains of patients has prion-like features, and we consider that the onset and progression of TDP-43 proteinopathy may be associated with the propagation of TDP-43 aggregates between neuronal cells. If this is so, suppressing the propagation of aggregated proteins may be a new therapeutic strategy for many neurodegenerative diseases.

EXPERIMENTAL PROCEDURES

Preparation of Detergent-Insoluble Fractions from Brains of Patients

Human brain tissues were obtained from Fukushimura Hospital, Aichi Medical University (Aichi, Japan), Shizuoka Institute of Epilepsy and Neurological Disorders (Shizuoka, Japan), and Tokyo Metropolitan Institute of Gerontology (Tokyo, Japan). This study was approved by the local research ethics committee of Tokyo Metropolitan Institute of Medical Science (approval No. 12-3). The subjects included four patients with ALS, one with FTLD-TDP type A, three with FTLD-TDP type C, one with dementia with Lewy bodies, and one with Pick's disease. All patients with ALS met the revised El Escorial criteria for ALS (Brooks, 1994) without dementia. All patients with FTLD-TDP met the clinical diagnostic criteria of FTLD (Neary et al., 1998), and TDP-43 subtypes were classified according to published guidelines (Mackenzie et al., 2011).

Brain samples (0.5 g) from patients with ALS, FTLD-TDP, or Pick's disease were each homogenized in 2.5 ml of homogenization buffer (HB: 10 mM Tris-HCl, pH 7.5 containing 0.8 M NaCl, 1 mM EGTA, 1 mM dithiothreitol). Sarkosyl was added to the lysates (final concentration: 1%), which were then incubated for 30 min at 37°C, and centrifuged at 12,000 *g* for 10 min at room temperature. The supernatant was further centrifuged at 100,000 *g* for 10 min at room temperature. The pellet was suspended in 2 ml PBS by sonication. Lysates were divided into four tubes (each 500 μL) and centrifuged at 100,000 *g* for 20 min at room temperature. The resulting pellets were used as the detergent-insoluble fraction (ppt).

For immuno-electron microscopy analyses, the detergent-insoluble fractions prepared from brains were placed on collodion-coated, 300-mesh copper grids and stained with anti-pS409/410 and 2% (v/v) phosphotungstate. Micrographs were recorded on a JEOL JEM-1400 electron microscope.

In ID experiments, mixtures of anti-pS409/410 and anti-TDP-43 polyclonal antibody (Proteintech; 2 μl each) were added to 20 μl of ALS ppt suspension

Please cite this article in press as: Nonaka et al., Prion-like Properties of Pathological TDP-43 Aggregates from Diseased Brains, Cell Reports (2013), http://dx.doi.org/10.1016/j.celrep.2013.06.007

Cell PRESS
Open ACCESS

in PBS, followed by addition of 10 μl of protein G-Sepharose (Sigma). After overnight incubation at 4°C, the supernatant was recovered. As a control, the other half of the lysate was incubated with a mixture of nonspecific mouse and rabbit immunoglobulin G (IgG; Cosmo Bio) and the same amount of protein G-Sepharose. An 8 μl aliquot of the supernatant was introduced into cells as described below.

In formic acid treatment, the detergent-insoluble fractions were suspended in 100 μl of 100% (v/v) formic acid (Nacalai Tesque) and incubated at room temperature for 30 min. After incubation, 900 μl of water was added and the mixtures were evaporated. The resulting residues were suspended in 500 μl of 0.1 M triethylammonium bicarbonate buffer (Fluka) and evaporated again. The residues were also suspended in 500 μl of water and centrifuged at 100,000 *g* for 20 min at room temperature. The resulting pellets were suspended in 100 μl of PBS and the mixtures were used for introduction experiments (see below).

Cell Culture and Transfection of Expression Plasmids

Human neuroblastoma SH-SY5Y cells obtained from ATCC were cultured in Dulbecco's modified Eagle's medium (DMEM)/F12 medium (Sigma-Aldrich) supplemented with 10% (v/v) fetal calf serum, penicillin-streptomycin-glutamine (Gibco), and MEM nonessential amino acids solution (Gibco). The cells were maintained at 37°C under a humidified atmosphere of 5% (v/v) CO_2 in air. They were grown to 50% confluence in six-well culture dishes for transient expression and then transfected with expression plasmids (usually 1 μg) using FuGENE6 (Roche) according to the manufacturer's instructions. Under our conditions, the efficiency of transfection using pEGFP-C1 vector was 20%–30%.

Introduction of Insoluble Proteins into Cells

Detergent-insoluble fractions prepared as described above were suspended in 150 μl PBS by sonication. Then 5 μg of insoluble fraction was mixed with 120 μl of Opti-MEM (Gibco), and 62.5 μl of Multifectam was added. After incubation for 30 min at room temperature, 62.5 μl of Opti-MEM was added and incubation was continued for 5 min at room temperature. Then, the mixtures were added to cells (mock cells or cells expressing HA-TDP-43, non-tagged TDP-43, or TDP-43 ΔNLS) and incubation was continued for 6 hr in a CO_2 incubator. After incubation, the medium was changed to fresh DMEM/F12 and culture was continued for the indicated period in each case. The cells were harvested and cellular proteins were differentially extracted and immunoblotted with the indicated antibodies, as previously described (Nonaka et al., 2010). Under our conditions, the efficiency of introduction of brain extracts was ~10%.

Confocal Microscopy

SH-SY5Y cells on coverslips were transfected with the indicated plasmids and cultured for 14 hr as described above. Then, the detergent-insoluble fraction was introduced and culture was continued for ~1–2 days. After fixation with 4% paraformaldehyde, cells were stained with the appropriate primary and secondary antibodies as described previously (Nonaka et al., 2010). Fluorescence was analyzed with a laser scanning confocal fluorescence microscope (LSM5 Pascal; Carl Zeiss). Confocal Z slices with an interval of 0.2 or 0.5 μm were obtained and reconstructed for three-dimensional observation using LSM5 Pascal v 4.0 software.

Cell Death Assay

Cell death assays were performed using a CytoTox 96 Non-Radioactive Cytotoxicity Assay Kit (Promega).

Assay of Proteasome Activity

In a GFP-reporter assay to monitor proteasome activity in cultured cells by confocal laser microscopy, SH-SY5Y cells that had been transfected with pcDNA3-HA-TDP-43 (1 μg) and GFP-CL1 (0.3 μg) using FuGENE6 and then treated with detergent-insoluble fraction of ALS brain were grown on coverslips for 2 days or treated with 0.1 μM MG132 overnight (Nonaka and Hasegawa, 2009; Nonaka et al., 2010). These cells were analyzed with the use of a laser-scanning confocal fluorescence microscope (LSM5Pascal; Carl Zeiss).

Coculture of Cells

SH-SY5Y cells transiently expressing DsRed (3 days after transfection) were mixed equally with cells expressing TDP-43 and treated with ALS ppt (3 days after introduction of ALS ppt). The cocultured cells were grown for a further 3 days, fixed with 4% paraformaldehyde, stained with anti-pS409/410 and TO-PRO-3, and observed under a laser-scanning confocal fluorescence microscope (LSM5Pascal; Carl Zeiss).

Preparation of Exosome Fractions

Exosome fractions were prepared from 4 ml of culture medium of cells expressing TDP-43, cells treated with ALS ppt, or cells transfected with both TDP-43 and ALS ppt, which had been cultured for 3 days after transfection, using an ExoQuick-TC kit from SBI according to the manufacturer's protocol. The exosome fractions were dissolved in 100 μl of SDS sample buffer and immunoblotted.

Statistical Analysis

Statistical analyses were performed using GraphPad Prism 4 software (GraphPad Software). Biochemical data were statistically analyzed using the unpaired, two-tailed Student's t test. A p value of ≤ 0.05 was considered to be statistically significant. For further details regarding the materials and methods used in this work, see Extended Experimental Procedures.

SUPPLEMENTAL INFORMATION

Supplemental Information includes Extended Experimental Procedures and three figures and can be found with this article online at http://dx.doi.org/10.1016/j.celrep.2013.06.007.

ACKNOWLEDGMENTS

We thank Makiko Yamashita and Masato Hosokawa for helpful comments. This work was supported by a Grant-in-Aid for Scientific Research (C) (JSPS KAKENHI 22500345 to T.N.), a Grant-in-Aid for Scientific Research (S) (JSPS KAKENHI 23228004 to M.H.) a Grant-in-Aid for Scientific Research (A) (JSPS KAKENHI 23240050 to M.H.), MHLW Grant (Number 12946221 to M.H.), a Grant-in-Aid for Scientific Research on Innovative Area "Brain Environment" (MEXT KAKENHI 24111556 to T.N.), and a grant from the Takeda Science Foundation (to T.N.).

Received: March 12, 2013
Revised: May 17, 2013
Accepted: June 6, 2013
Published: July 3, 2013

REFERENCES

Arai, T., Hasegawa, M., Akiyama, H., Ikeda, K., Nonaka, T., Mori, H., Mann, D., Tsuchiya, K., Yoshida, M., Hashizume, Y., and Oda, T. (2006). TDP-43 is a component of ubiquitin-positive tau-negative inclusions in frontotemporal lobar degeneration and amyotrophic lateral sclerosis. Biochem. Biophys. Res. Commun. *351*, 602–611.

Arai, T., Hasegawa, M., Nonoka, T., Kametani, F., Yamashita, M., Hosokawa, M., Niizato, K., Tsuchiya, K., Kobayashi, Z., Ikeda, K., et al. (2010). Phosphorylated and cleaved TDP-43 in ALS, FTLD and other neurodegenerative disorders and in cellular models of TDP-43 proteinopathy. Neuropathology *30*, 170–181.

Bence, N.F., Sampat, R.M., and Kopito, R.R. (2001). Impairment of the ubiquitin-proteasome system by protein aggregation. Science *292*, 1552–1555.

Bigio, E.H., Wu, J.Y., Deng, H.X., Bit-Ivan, E.N., Mao, Q., Ganti, R., Peterson, M., Siddique, N., Geula, C., Siddique, T., and Mesulam, M. (2013). Inclusions in frontotemporal lobar degeneration with TDP-43 proteinopathy (FTLD-TDP) and amyotrophic lateral sclerosis (ALS), but not FTLD with FUS proteinopathy (FTLD-FUS), have properties of amyloid. Acta Neuropathol. *125*, 463–465.

Braak, H., and Braak, E. (1991). Neuropathological stageing of Alzheimer-related changes. Acta Neuropathol. *82*, 239–259.

Please cite this article in press as: Nonaka et al., Prion-like Properties of Pathological TDP-43 Aggregates from Diseased Brains, Cell Reports (2013), http://dx.doi.org/10.1016/j.celrep.2013.06.007

Braak, H., Del Tredici, K., Rüb, U., de Vos, R.A., Jansen Steur, E.N., and Braak, E. (2003). Staging of brain pathology related to sporadic Parkinson's disease. Neurobiol. Aging *24*, 197–211.

Brooks, B.R. (1994). El Escorial World Federation of Neurology criteria for the diagnosis of amyotrophic lateral sclerosis. Subcommittee on Motor Neuron Diseases/Amyotrophic Lateral Sclerosis of the World Federation of Neurology Research Group on Neuromuscular Diseases and the El Escorial "Clinical Limits of Amyotrophic Lateral Sclerosis" workshop contributors. J. Neurol. Sci. *124(Suppl)*, 96–107.

Budini, M., Buratti, E., Stuani, C., Guarnaccia, C., Romano, V., De Conti, L., and Baralle, F.E. (2012). Cellular model of TAR DNA binding protein 43 (TDP-43) aggregation based on its C-terminal Q/N rich region. J. Biol. Chem. *287*, 7512–7525.

Buratti, E., and Baralle, F.E. (2009). The molecular links between TDP-43 dysfunction and neurodegeneration. Adv. Genet. *66*, 1–34.

Buratti, E., Dörk, T., Zuccato, E., Pagani, F., Romano, M., and Baralle, F.E. (2001). Nuclear factor TDP-43 and SR proteins promote in vitro and in vivo CFTR exon 9 skipping. EMBO J. *20*, 1774–1784.

Clavaguera, F., Bolmont, T., Crowther, R.A., Abramowski, D., Frank, S., Probst, A., Fraser, G., Stalder, A.K., Beibel, M., Staufenbiel, M., et al. (2009). Transmission and spreading of tauopathy in transgenic mouse brain. Nat. Cell Biol. *11*, 909–913.

de Calignon, A., Polydoro, M., Suárez-Calvet, M., William, C., Adamowicz, D.H., Kopeikina, K.J., Pitstick, R., Sahara, N., Ashe, K.H., Carlson, G.A., et al. (2012). Propagation of tau pathology in a model of early Alzheimer's disease. Neuron *73*, 685–697.

Desplats, P., Lee, H.J., Bae, E.J., Patrick, C., Rockenstein, E., Crews, L., Spencer, B., Masliah, E., and Lee, S.J. (2009). Inclusion formation and neuronal cell death through neuron-to-neuron transmission of alpha-synuclein. Proc. Natl. Acad. Sci. USA *106*, 13010–13015.

Fevrier, B., Vilette, D., Archer, F., Loew, D., Faigle, W., Vidal, M., Laude, H., and Raposo, G. (2004). Cells release prions in association with exosomes. Proc. Natl. Acad. Sci. USA *101*, 9683–9688.

Frost, B., Jacks, R.L., and Diamond, M.I. (2009). Propagation of tau misfolding from the outside to the inside of a cell. J. Biol. Chem. *284*, 12845–12852.

Furukawa, Y., Kaneko, K., Watanabe, S., Yamanaka, K., and Nukina, N. (2011). A seeding reaction recapitulates intracellular formation of Sarkosyl-insoluble transactivation response element (TAR) DNA-binding protein-43 inclusions. J. Biol. Chem. *286*, 18664–18672.

Goedert, M., Clavaguera, F., and Tolnay, M. (2010). The propagation of prion-like protein inclusions in neurodegenerative diseases. Trends Neurosci. *33*, 317–325.

Gousset, K., Schiff, E., Langevin, C., Marijanovic, Z., Caputo, A., Browman, D.T., Chenouard, N., de Chaumont, F., Martino, A., Enninga, J., et al. (2009). Prions hijack tunnelling nanotubes for intercellular spread. Nat. Cell Biol. *11*, 328–336.

Guo, W., Chen, Y., Zhou, X., Kar, A., Ray, P., Chen, X., Rao, E.J., Yang, M., Ye, H., Zhu, L., et al. (2011). An ALS-associated mutation affecting TDP-43 enhances protein aggregation, fibril formation and neurotoxicity. Nat. Struct. Mol. Biol. *18*, 822–830.

Hasegawa, M., Arai, T., Nonaka, T., Kametani, F., Yoshida, M., Hashizume, Y., Beach, T.G., Buratti, E., Baralle, F., Morita, M., et al. (2008). Phosphorylated TDP-43 in frontotemporal lobar degeneration and amyotrophic lateral sclerosis. Ann. Neurol. *64*, 60–70.

Hasegawa, M., Nonaka, T., Tsuji, H., Tamaoka, A., Yamashita, M., Kametani, F., Yoshida, M., Arai, T., and Akiyama, H. (2011). Molecular dissection of TDP-43 proteinopathies. J. Mol. Neurosci. *45*, 480–485.

Igaz, L.M., Kwong, L.K., Chen-Plotkin, A., Winton, M.J., Unger, T.L., Xu, Y., Neumann, M., Trojanowski, J.Q., and Lee, V.M. (2009). Expression of TDP-43 C-terminal fragments in vitro recapitulates pathological features of TDP-43 proteinopathies. J. Biol. Chem. *284*, 8516–8524.

Kordower, J.H., Chu, Y., Hauser, R.A., Freeman, T.B., and Olanow, C.W. (2008). Lewy body-like pathology in long-term embryonic nigral transplants in Parkinson's disease. Nat. Med. *14*, 504–506.

Li, J.Y., Englund, E., Holton, J.L., Soulet, D., Hagell, P., Lees, A.J., Lashley, T., Quinn, N.P., Rehncrona, S., Björklund, A., et al. (2008). Lewy bodies in grafted neurons in subjects with Parkinson's disease suggest host-to-graft disease propagation. Nat. Med. *14*, 501–503.

Liu, L., Drouet, V., Wu, J.W., Witter, M.P., Small, S.A., Clelland, C., and Duff, K. (2012). Trans-synaptic spread of tau pathology in vivo. PLoS ONE *7*, e31302.

Luk, K.C., Song, C., O'Brien, P., Stieber, A., Branch, J.R., Brunden, K.R., Trojanowski, J.Q., and Lee, V.M. (2009). Exogenous alpha-synuclein fibrils seed the formation of Lewy body-like intracellular inclusions in cultured cells. Proc. Natl. Acad. Sci. USA *106*, 20051–20056.

Luk, K.C., Kehm, V., Carroll, J., Zhang, B., O'Brien, P., Trojanowski, J.Q., and Lee, V.M. (2012a). Pathological α-synuclein transmission initiates Parkinson-like neurodegeneration in nontransgenic mice. Science *338*, 949–953.

Luk, K.C., Kehm, V.M., Zhang, B., O'Brien, P., Trojanowski, J.Q., and Lee, V.M. (2012b). Intracerebral inoculation of pathological α-synuclein initiates a rapidly progressive neurodegenerative α-synucleinopathy in mice. J. Exp. Med. *209*, 975–986.

Mackenzie, I.R., Neumann, M., Baborie, A., Sampathu, D.M., Du Plessis, D., Jaros, E., Perry, R.H., Trojanowski, J.Q., Mann, D.M., and Lee, V.M. (2011). A harmonized classification system for FTLD-TDP pathology. Acta Neuropathol. *122*, 111–113.

Masuda-Suzukake, M., Nonaka, T., Hosokawa, M., Oikawa, T., Arai, T., Akiyama, H., Mann, D.M.A., and Hasegawa, M. (2013). Prion-like spreading of pathological α-synuclein in brain. Brain *136*, 1128–1138.

Neary, D., Snowden, J.S., Gustafson, L., Passant, U., Stuss, D., Black, S., Freedman, M., Kertesz, A., Robert, P.H., Albert, M., et al. (1998). Frontotemporal lobar degeneration: a consensus on clinical diagnostic criteria. Neurology *51*, 1546–1554.

Neumann, M., Sampathu, D.M., Kwong, L.K., Truax, A.C., Micsenyi, M.C., Chou, T.T., Bruce, J., Schuck, T., Grossman, M., Clark, C.M., et al. (2006). Ubiquitinated TDP-43 in frontotemporal lobar degeneration and amyotrophic lateral sclerosis. Science *314*, 130–133.

Nonaka, T., and Hasegawa, M. (2009). A cellular model to monitor proteasome dysfunction by alpha-synuclein. Biochemistry *48*, 8014–8022.

Nonaka, T., Kametani, F., Arai, T., Akiyama, H., and Hasegawa, M. (2009). Truncation and pathogenic mutations facilitate the formation of intracellular aggregates of TDP-43. Hum. Mol. Genet. *18*, 3353–3364.

Nonaka, T., Watanabe, S.T., Iwatsubo, T., and Hasegawa, M. (2010). Seeded aggregation and toxicity of alpha-synuclein and tau: cellular models of neurodegenerative diseases. J. Biol. Chem. *285*, 34885–34898.

Pesiridis, G.S., Lee, V.M., and Trojanowski, J.Q. (2009). Mutations in TDP-43 link glycine-rich domain functions to amyotrophic lateral sclerosis. Hum. Mol. Genet. *18*(R2), R156–R162.

Polymenidou, M., and Cleveland, D.W. (2011). The seeds of neurodegeneration: prion-like spreading in ALS. Cell *147*, 498–508.

Ren, P.H., Lauckner, J.E., Kachirskaia, I., Heuser, J.E., Melki, R., and Kopito, R.R. (2009). Cytoplasmic penetration and persistent infection of mammalian cells by polyglutamine aggregates. Nat. Cell Biol. *11*, 219–225.

Sephton, C.F., Good, S.K., Atkin, S., Dewey, C.M., Mayer, P., 3rd, Herz, J., and Yu, G. (2010). TDP-43 is a developmentally regulated protein essential for early embryonic development. J. Biol. Chem. *285*, 6826–6834.

Snowden, J.S., Neary, D., and Mann, D.M. (2002). Frontotemporal dementia. Br. J. Psychiatry *180*, 140–143.

Tsuji, H., Arai, T., Kametani, F., Nonaka, T., Yamashita, M., Suzukake, M., Hosokawa, M., Yoshida, M., Hatsuta, H., Takao, M., et al. (2012). Molecular analysis and biochemical classification of TDP-43 proteinopathy. Brain *135*, 3380–3391.

Wu, L.S., Cheng, W.C., Hou, S.C., Yan, Y.T., Jiang, S.T., and Shen, C.K. (2010). TDP-43, a neuro-pathosignature factor, is essential for early mouse embryogenesis. Genesis *48*, 56–62.

Zhang, Y.J., Xu, Y.F., Cook, C., Gendron, T.F., Roettges, P., Link, C.D., Lin, W.L., Tong, J., Castanedes-Casey, M., Ash, P., et al. (2009). Aberrant cleavage of TDP-43 enhances aggregation and cellular toxicity. Proc. Natl. Acad. Sci. USA *106*, 7607–7612.

nature COMMUNICATIONS

ARTICLE

Received 2 Nov 2013 | Accepted 5 Feb 2014 | Published 28 Feb 2014

DOI: 10.1038/ncomms4386

Decreased CALM expression reduces Aβ42 to total Aβ ratio through clathrin-mediated endocytosis of γ-secretase

Kunihiko Kanatsu[1,*], Yuichi Morohashi[1,2,*], Mai Suzuki[3], Hiromasa Kuroda[1], Toshio Watanabe[3], Taisuke Tomita[1,2] & Takeshi Iwatsubo[1,2,4]

A body of evidence suggests that aberrant metabolism of amyloid-β peptide (Aβ) underlies the aetiology of Alzheimer disease (AD). Recently, a single-nucleotide polymorphism in phosphatidylinositol binding clathrin assembly protein (*PICALM/CALM*) gene, which encodes a protein implicated in the clathrin-mediated endocytosis, was identified as a genetic protective factor for AD, although its mechanistic details have little been explored. Here we show that loss of CALM leads to the selective decrease in the production ratio of the pathogenic Aβ species, Aβ42. Active form of γ-secretase is constitutively endocytosed via the clathrin-mediated pathway in a CALM dependent manner. Alteration in the rate of clathrin-mediated endocytosis of γ-secretase causes a shift in its steady-state localization, which consequently impacts on the production ratio of Aβ42. Our study identifies CALM as an endogenous modulator of γ-secretase activity by regulating its endocytosis and also as an excellent target for Aβ42-lowering AD therapeutics.

[1] Department of Neuropathology and Neuroscience, Graduate School of Pharmaceutical Sciences, The University of Tokyo, Tokyo 113-0033, Japan. [2] Core Research for Evolutional Science and Technology, Japan Science and Technology Agency, Tokyo 113-0033, Japan. [3] Department of Biological Science, Graduate School of Humanities and Sciences, Nara Women's University, Nara 630-8506, Japan. [4] Department of Neuropathology, Graduate School of Medicine, The University of Tokyo, Tokyo 113-0033, Japan. * These authors contributed equally to this work. Correspondence and requests for materials should be addressed to T.T. (email: taisuke@mol.f.u-tokyo.ac.jp).

Amyloid-β peptide (Aβ) deposited in the brains of patients with Alzheimer disease (AD) is derived from amyloid-β precursor protein (APP) through sequential proteolytic cleavages by BACE1 and γ-secretase[1]. Cleavage of APP by γ-secretase occurs at multiple sites within the transmembrane domain to generate Aβ species with a carboxyl-terminal heterogeneity[2,3]. Two major forms of Aβ have distinct C termini ending at the 40th and 42nd residues (Aβ40 and Aβ42, respectively). Aβ42 is the most aggregable and massively deposited species in the brains of patients with AD and Down's syndrome[4]. Mutations linked to familial AD (FAD) have been identified in genes encoding APP as well as presenilin (PSEN, hereafter referred to as PS), the latter being the catalytic subunit of the γ-secretase complex[5]. Previous studies revealed that several FAD mutations lead to an increased proportion of Aβ42, strongly implicating Aβ42 in the pathogenesis of AD. However, it still remains unclear whether the Aβ42 production is altered in sporadic AD as well as in ageing. Also, the regulatory mechanism that determines the γ-cleavage site remains elusive. γ-Secretase is a multimeric membrane protein complex composed of PS, nicastrin (Nct), Aph-1 and Pen-2 (refs 3,6). γ-Secretase activity is suggested to be broadly distributed between the *trans*-Golgi network and cell surface[7,8]. But recent studies including fly genetics regarding Notch processing revealed the prevalence of γ-secretase activity in late endosomes/multivesicular bodies (MVB) and lysosomes[9,10]. Thus, endocytic trafficking of γ-secretase might play an important role for Aβ generation, while its precise subcellular localization as well as the molecular details of the trafficking machinery of the endogenous γ-secretase still remains mostly unclear.

PICALM gene has been identified as one of the genetic risk/protective factors for AD by the genome-wide association studies in late-onset AD patients[11]. Large meta-analysis of 74,046 individuals[12] revealed that carriers with minor allele (A) of rs10792832 near *PICALM* gene showed a decreased risk for AD with an odds ratio of 0.85–0.89. *PICALM* encodes a protein called CALM (*C*lathrin *A*ssembly *L*ymphoid *M*yeloid leukemia[13]), which has a phosphatidylinositol 4,5-biphosphate ($PtdIns(4,5)P_2$) binding ANTH domain at its N terminus, along with AP-2/clathrin binding motifs in the C-terminal region, indicating that CALM functions in the initial step of clathrin-mediated endocytosis by facilitating the proper formation of clathrin-coated pits[14,15]. More recently, CALM has been shown to interact directly with some of the endosomal R-SNARE proteins (that is, VAMP2, VAMP3 and VAMP8) via its ANTH domain and regulate their clathrin-dependent endocytosis[16], suggesting its additional role in the direct recognition of endocytic cargo proteins. With regard to the relationship between CALM and the aetiology of AD, some genome-wide association studies have shown a genetic interaction of *PICALM* with *ApoE*, implying a possible involvement of CALM in the process of Aβ production/deposition[17]. Using yeast genetics and AD model mice, CALM has recently been implicated in the endocytosis of secreted Aβ and APP; however, its mechanistic details were mostly unknown[18,19].

Here we find that CALM regulates the endocytosis and subcellular localization of the γ-secretase and impacts on the production ratio of Aβ42. Our data raise the possibility that CALM is an endogenous γ-secretase modulator and that its variant affects the onset of AD by altering the Aβ42 production ratio in an opposite manner to that by FAD-linked mutations in *APP* and *PS* genes.

Results

Expression level of CALM is correlated with Aβ42 ratio. To analyse the effect of CALM on Aβ metabolism *in vivo*, we measured Aβ levels in the brains of *Picalm*-mutant mice[20]. Previous studies have shown that changes in endogenous murine brain Aβ by overexpression/knock-in of FAD mutant PS1 (refs 21–23), or knockout of PS1 (ref. 24) or BACE1 (refs 25,26) occurred in a similar manner to those observed in congenic mice crossed with human APP transgenic mice. As homozygous knockout mice show significant growth defect and die shortly after birth, we opted to use heterozygous $Picalm^{+/-}$ mice, which are viable with no obvious defect. Strikingly, we found that the Aβ42/total Aβ ratio, that is, proportion of Aβ42 to total Aβ (= Aβ40 + Aβ42), in the soluble fraction of brain lysate of $Picalm^{+/-}$ mice was significantly decreased by ~20% compared with that of wild-type mice (Fig. 1a,b). Notably, that protein expression levels of the γ-secretase components (Nct and C-terminal fragment (CTF) of PS1) in the brains of $Picalm^{+/-}$ mice were increased (Fig. 1c–e). To investigate whether CALM affects the generation process of Aβ42, we measured Aβ secreted from cultured cells in the medium. In good agreement with the result from mouse brains, RNAi against *Picalm* in Neuro2a (N2a) cells, which caused near-complete depletion of CALM protein, resulted in a statistically significant reduction in Aβ42/total Aβ ratio in the secreted Aβ (Fig. 2a–e) regardless of the siRNA sequences (Fig. 2d) or APP species (Fig. 2e), suggesting that CALM expression levels had an impact on Aβ42 production ratio. In addition, we observed the accumulation of APP full-length (fl) protein and CTF, although APP levels were almost comparable in brains of wild-type and $Picalm^{+/-}$ mice (see Fig. 1). Next we examined the effects of overexpression of CALM in N2a cells. Alternative splicing of CALM mRNA with an internal deletion of 50 amino-acid residues was reported previously (CALM-S)[13,14], although the large isoform of CALM (CALM-L) was expressed as the major species in N2a cells. However, overexpression of neither CALM-L nor CALM-S in N2a cells affected the Aβ production, supporting the notion that the formation of CALM protein complex in concert with AP-2 and clathrin heavy chain is required for the regulation of clathrin-mediated endocytosis[14,15] (Fig. 2f–h). As Aβ generation is a multi-step process, it is critical to determine which step in the Aβ generation is affected by CALM depletion. The enzymatic activity of BACE1 in the $Picalm^{+/-}$ brain was almost comparable to that in wild-type mice (Fig. 3a). We then measured Aβ secretion from CALM-depleted HeLa cells expressing APP C99, a direct γ-secretase substrate[27]. A decrease in Aβ42/total Aβ ratio was also observed (Fig. 3b–d), suggesting that the loss of CALM affects γ-secretase-mediated APP processing. These data suggest that the cellular amount of CALM protein correlates with the ratio of Aβ42 production at the level of γ-secretase cleavage.

CALM regulates the endocytosis of the γ-secretase complex. The result that the level of γ-secretase components was increased in $Picalm^{+/-}$ mouse brains prompted us to speculate that CALM might affect the endocytosis and metabolism of γ-secretase. In fact, we found the accumulation of mature Nct in the lysate of CALM RNAi cells. Cell surface biotinylation experiment revealed that CALM knockdown significantly increased the levels of mature Nct at the cell surface (Fig. 4). However, the intracellular localization and trafficking of γ-secretase have been under debate for years; earlier reports suggest that γ-secretase localizes at TGN, plasma membrane, endosomes and lysosomes[9,28–30]. Importantly, a detailed cell biological study of γ-secretase trafficking has been hampered because of the lack of an appropriate probe, which can specifically recognize an active, fully-assembled γ-secretase. Recently, we have developed a mouse monoclonal antibody A5226A against mature human Nct that is specifically incorporated in active γ-secretase[31].

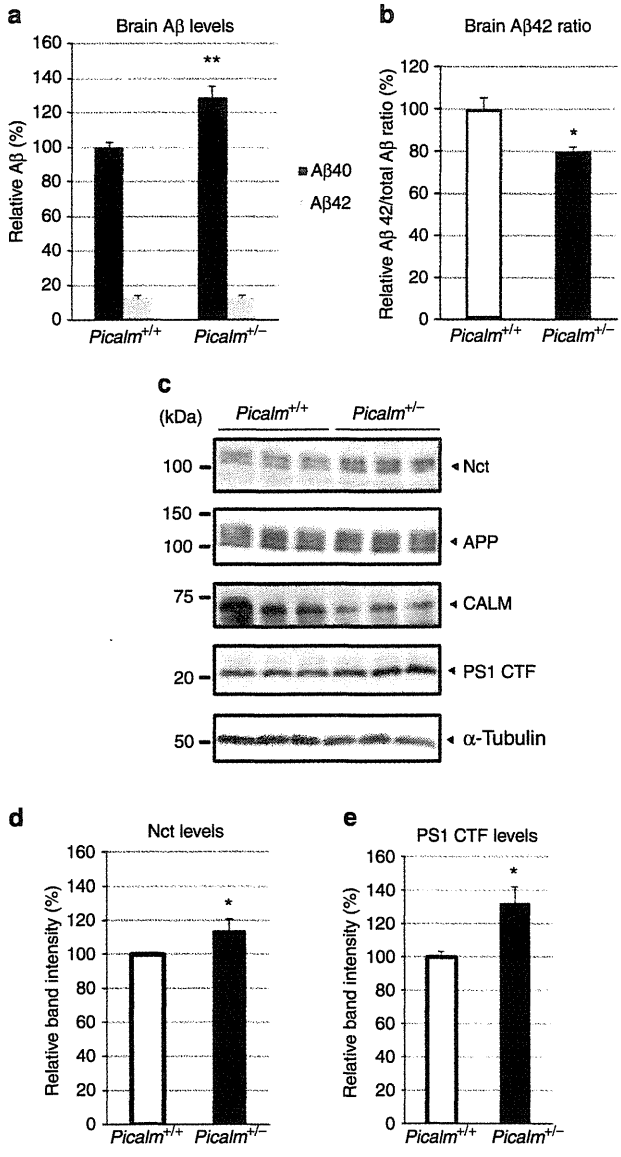

Figure 1 | Brain Aβ42 ratio is reduced in the *Picalm*$^{+/-}$ mouse brain. (**a**) Relative levels of Aβ40 and Aβ42 in Tris-soluble fraction of brains from 5-month-old *Picalm*$^{+/-}$ or wild-type mice were quantitated by sandwich ELISAs ($n=7$, mean ± s.e.m. $^{**}P<0.005$ by student's *t*-test). (**b**) Relative Aβ42/total Aβ ratio in experiment (**a**) ($n=7$, mean ± s.e.m., $^{*}P<0.05$ by Student's *t*-test). (**c**) Western blot analysis of Tris-soluble fraction of brains from 5-month-old *Picalm*$^{+/-}$ or wild-type mice with antibodies against Nct, APP, CALM, PS1 CTF and α-tubulin. Full size blots can be found in Supplementary Fig. 1. (**d**,**e**) Quantification of band intensities of total Nct (**d**) and PS1 CTF (**e**) in (**c**) ($n=3$, mean ± s.e.m., $^{*}P<0.05$ by Student's *t*-test).

Immunofluorescence analysis using this antibody with HeLa cells revealed that γ-secretase mostly colocalized with the late endosomal/lysosomal marker LAMP1, confirming some of the findings in the previous reports (Fig. 5a)[7,9]. Intriguingly, CALM depletion caused cell surface accumulation and less prominent late endosome localization of γ-secretase. In addition, anti-LAMP 1 staining became dispersed, suggesting that the loss of CALM caused disorganized late endosomes (Fig. 5a) by an impaired endocytosis of VAMP8 that is important for the fusion of late endosomes, as reported recently[16]. To investigate this further, we set up an A5226A uptake assay to monitor endocytosis of γ-secretase. In the control cells, γ-secretase is internalized slowly and started to accumulate in EEA1-positive early endosomes after 20 min of chase period and stayed there at 60 min of chase (asterisks, Fig. 5b). Further chase visualized γ-secretase in EEA1-negative late endosomes at 480 min (Fig. 5c). Strikingly, A5226A uptake was markedly diminished in CALM-depleted cells (Fig. 5b). The majority of A5226A-labelled γ-secretase stayed at the cell surface even after 60 min of chase period (arrowheads, Fig. 5b) and only a minor portion reached the EEA1-positive early endosomes. The endocytosis of γ-secretase was blocked also by treatment with Pitstop 2 (arrowheads, Fig. 5d), a compound that binds to the terminal domain of clathrin heavy chain and perturbs clathrin-coated pit dynamics without affecting pit assembly nor the sequestration of the cargos[32]. Consistent with these results, a substantial colocalization of A5226A and CALM was detected at the cell surface of Pitstop 2-treated HeLa cells, a finding indicative of accumulation of γ-secretase in clathrin-coated pits in Pitstop 2-treated HeLa cells (Fig. 5e), suggesting that γ-secretase is internalized by clathrin-mediated endocytosis in a CALM-dependent manner.

This finding was consistent with the biochemical data obtained by surface biotinylation-based endocytosis assay using a cleavable biotin reagent, NHS-SS-biotin. Sodium 2-mercaptoethanesulfonate (MeSNa) treatment causes the stripping of NHS-SS-biotin from the proteins at the cell surface, but not the internalized proteins (Fig. 6a). Using this reagent, the amounts of biotinylated proteins that are protected by internalization can be quantitated by pull down using streptavidin beads as 'endocytosed proteins' after appropriate chase periods[33]. The amount of internalized pool of MeSNa-labelled Nct in the control cells was significantly higher than that in CALM siRNA-treated cells (Fig. 6b–e). We also found that the levels of Nct in the brains of *Picalm*$^{+/-}$ mice and CALM-depleted cells were significantly higher than those in controls (Figs 1 and 4), indicating that Nct is accumulated possibly as a consequence of delayed CALM-dependent endocytosis and subsequent degradation. Previous report suggested that the endocytosis of APP and Aβ production in N2a cells overexpressing human APP was affected by CALM knockdown[19]. Importantly, cell surface levels of APP is regulated not only by endocytosis, but extracellular shedding by α-secretase. However, CALM knockdown caused a very limited effect on the amount of endocytosed MeSNa-labelled APP from the cell surface of HT1080 and N2a cells even under GM6001 treatment that inhibits shedding at the cell surface (Fig. 6c,e). These data suggest that endocytosis of endogenous APP is not regulated by CALM and that overexpression might have caused an overflow of exogenous APP into CALM-regulated clathrin-coated pits. Supporting this notion, reduction in total Aβ secretion by *Picalm* RNAi from overexpressed human APP (34.4% from stable expression, 74.4% from transient expression of non-target RNAi) was greater than that from endogenous murine APP in N2a cells (26.4% of non-target RNAi) (Fig. 6f). Recently, it has been reported that AP-2 and CALM bind to LC3 to facilitate the clearance of APP CTF by autophagy[34]. We examined whether APP is involved in the endocytosis of the γ-secretase by knockdown of endogenous APP. We performed the A5226A incorporation assay in APP-, CALM- and APP/CALM-knockdown cells (Fig. 7). Depletion of APP expression did not affect the endocytic transport of the γ-secretase. These data suggest that APP and its binding proteins are not involved in the endocytosis of γ-secretase by CALM.

CALM has been shown to regulate the endocytosis of a subset of membrane proteins as its cargo[14,20,35–37]. In regard to the recognition of the cargo, it has recently been shown that VAMP8,

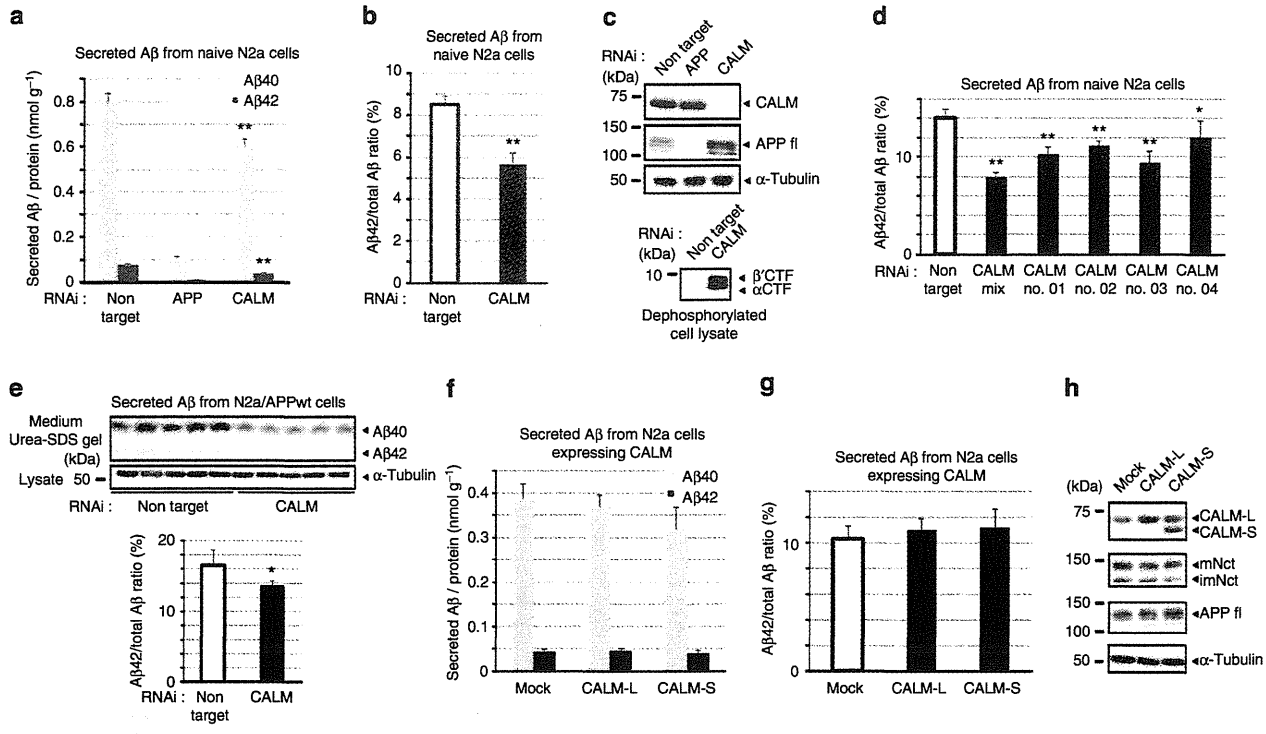

Figure 2 | Knockdown of CALM reduced Aβ42 ratio in secreted Aβ. (**a**) Levels of Aβ40 and Aβ42 secreted from N2a cells treated with non-target, APP o CALM siRNA duplex ($n=6$, mean ± s.e.m., $^{**}P<0.005$ by Student's t-test). (**b**) Aβ42/total Aβ ratio in experiment (**a**) ($n=6$, mean ± s.e.m., $^{**}P<0.00$ by Student's t-test). (**c**) N2a cells treated with siRNA duplexes were analysed by western blotting with antibodies against CALM, APP and α-tubulin. (**d**) Aβ42/total Aβ ratio in secreted Aβ in conditioned medium from N2a cells transfected with siRNAs against CALM with different target sequences. (**e**) Western blot analysis of the conditioned media and lysates from N2a cells stably expressing human APP by antibodies against human Aβ and α-tubuli antibody, respectively (Top panel). Aβ42/total Aβ ratio was calculated in bottom panel ($n=6$, mean ± s.e.m., $^{*}P<0.05$ by student's t-test). (**f**) Levels o Aβ40 and Aβ42 secreted from N2a cells transiently expressed with CALM-L or S ($n=6$, mean ± s.e.m). (**g**) Aβ42/total Aβ ratio in experiment (**f**) ($n=6$, mean ± s.e.m., $^{**}P<0.005$ by Student's t-test). (**h**) N2a cell lysates in experiment (**f**) were analysed by western blotting with antibodies against CALM, Nct, APP and α-tubulin (mNct, mature Nct; imNct, immature Nct). Full size blots for (**c**), (**e**) and (**h**) can be found in Supplementary Fig. 1.

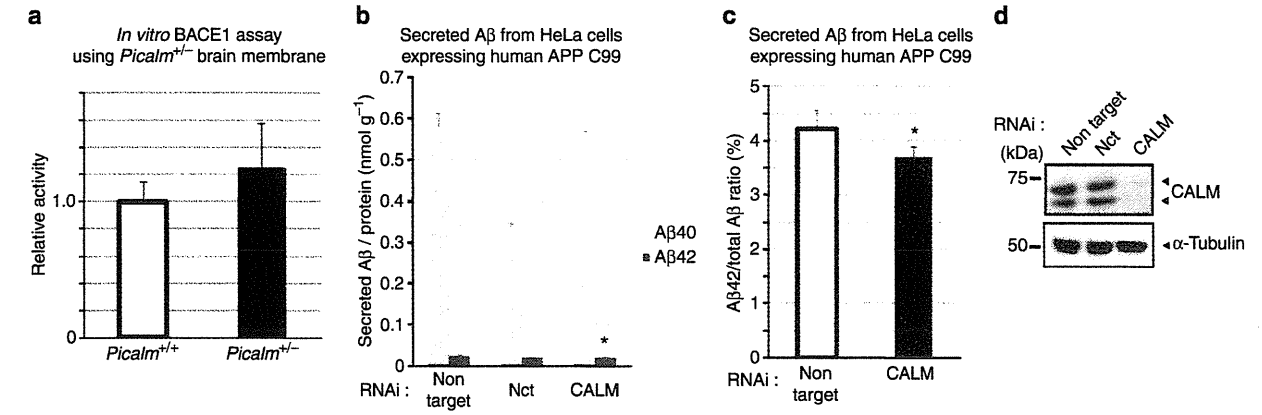

Figure 3 | CALM modulates the γ-secretase cleavage. (**a**) Relative BACE1 activity in the membrane fractions of wild-type or *Picalm*$^{+/-}$ mice brains. FRET-based BACE1 synthetic substrate was incubated with membrane fraction for 6 h, and then the fluorescence was measured ($n=3$, mean ± s.e.m). (**b**) Levels of Aβ40 and Aβ42 secreted from HeLa cells expressing APP C99 treated with non-target, Nct or CALM siRNA duplexes ($n=6$, mean ± s.e.m., $^{*}P<0.05$ by Student's t-test). (**c**) Aβ42/total Aβ ratio in experiment (**b**) ($n=6$, mean ± s.e.m., $^{*}P<0.05$ by Student's t-test). (**d**) HeLa cells treated with non-target, Nct, or CALM siRNA duplexes were analysed by western blotting with antibodies against CALM and α-tubulin. Full size blots can be found in the Supplementary Fig. 1.

one of the R-SNARE proteins, binds directly to the C-terminal edge of ANTH domain and is internalized in a CALM-dependent manner[16]. To test the possibility that CALM also directly recognizes γ-secretase as an endocytic cargo, we carried out ar *in vitro* binding experiment using GST-fused recombinant CALM proteins encoding an N-terminal PtdIns(4,5)P_2 binding ANTH

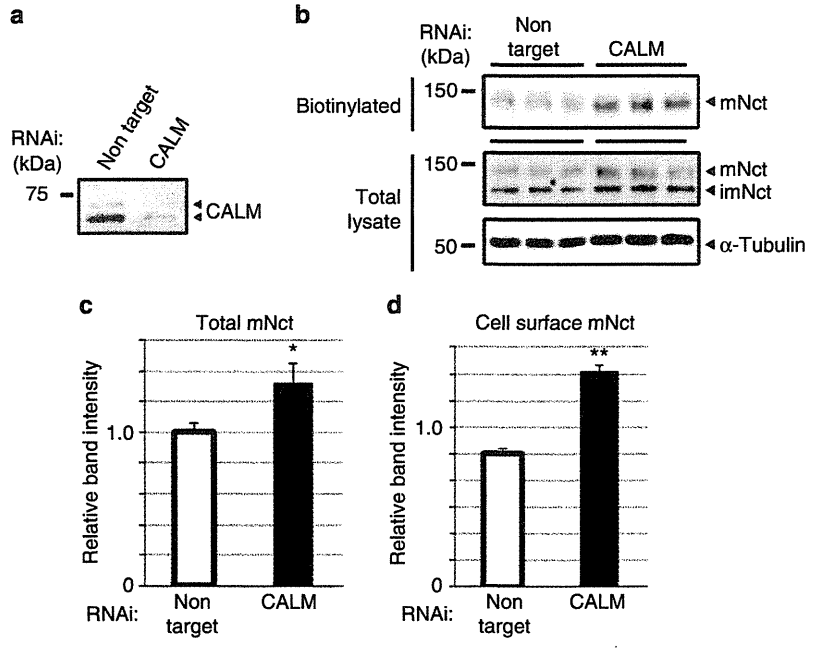

Figure 4 | CALM knockdown increases the expression levels of mature Nct. (**a**) HT1080 human fibrosarcoma cells treated with non-target or CALM were analysed by western blot. (**b**) Cell surface of HT1080 cells were biotinylated by NHS-SS-Biotin, and labelled proteins were selectively pulled down by streptavidin beads (mNct, mature Nct; imNct, immature Nct). (**c**,**d**) Quantification of band intensities of total mNct (**c**) and cell surface mNct (**d**) in (**b**) ($n=3$, mean ± s.e.m., $^*P<0.05$, $^{**}P<0.005$ by Student's t-test). Full size blots for (**a**) and (**b**) can be found in the Supplementary Fig. 1.

domain or the C-terminal region, which contains multiple clathrin and AP-2 binding motifs (ΔN) (Fig. 8a). We confirmed that VAMP8 as well as AP-2 specifically interacted with the recombinant ANTH domain and ΔN protein of CALM, respectively (Fig. 8b). Unexpectedly, AP-2 also interacted with the ANTH domain, raising the possibility that this region contains a novel AP-2 binding domain. In this condition, we found that endogenous Nct also bound to the ANTH domain, but not with the ΔN protein (Fig. 8b). The majority of GST-ANTH bound Nct was in its immature form, which represents the Nct species residing at ER. However, this band was not present in lysates from fibroblast of *Ncstn* knockout mice, and detected upon transfection of human Nct-V5, indicating that this polypeptide is Nct (Fig. 8c). In addition, we did observe the binding of mature Nct that locates at the cell surface (see Fig. 8c–e and discussed below). As Nct initially forms a subcomplex with Aph-1 and then binds to the C terminus of PS during the assembly process of γ-secretase[6,7], it is possible that Nct indirectly interacts with the ANTH domain through other subunits. However, interaction of Nct with recombinant ANTH domain was also observed in the lysates of fibroblasts lacking PS or Aph-1, indicating that CALM directly recognizes Nct as an endocytic cargo in the γ-secretase complex (Fig. 8d). Notably, VAMP8 knockdown caused no difference, rather, a slight increase in the amount of Nct associated with the ANTH domain, suggesting a possible competition between Nct and VAMP8 for their binding to the ANTH domain (Fig. 8e). Taken together, for the first time, we have shown that γ-secretase is constitutively internalized via the clathrin-dependent pathway as the endocytic cargo of CALM (Fig. 8f).

Aβ42 production ratio is increased by acidic pH. To test whether loss of CALM directly affects the enzymatic function of γ-secretase, we performed an *in vitro* γ-secretase assay using detergent-solubilized membrane fractions from CALM-depleted cells (Fig. 9). We observed no decrease in the Aβ42/total Aβ ratio of the *de novo* generated Aβ, suggesting that the intrinsic enzymatic activity of γ-secretase was not affected by CALM knockdown. Then we turned our attention to the finding that the localization of γ-secretase changed upon depletion of CALM. It led us to speculate that γ-secretase activity was affected by its altered subcellular localization. To explore this possibility, we took a pharmacological approach utilizing YM201636, which inhibits the phosphatidylinositol 3-phosphate 5-kinase Pikfyve. Pikfyve phosphorylates PtdIns3P to generate PtdIns(3,5)P_2 and is responsible for the maturation of early endosomes/multivesicular bodies into the degradative late endosomes/lysosomes[38]. YM201636 treatment caused increased vacuolation and redistribution of EEA1 and LAMP1 as reported previously[38] (Fig. 10a). Intriguingly, YM201636 caused a reduction in the Aβ42/total Aβ ratio in the secreted Aβ as well as accumulation of mature Nct, APP full length and CTF, similarly to those in CALM-depleted cells (Fig. 10b–d). Consistent with this, knockdown of YM201636-target kinase Pikfyve also reduced the Aβ42/total Aβ ratio, along with accumulation of APP and CTFs (Fig. 10e–g), suggesting that Pikfyve-mediated late endosomal maturation is closely involved in the Aβ42 production. However, incubation of the membrane fraction from YM201636-treated cells showed no difference in Aβ42/total Aβ ratio in *de novo*-generated Aβ (Fig. 10h), suggesting that the decrease in Aβ42/total Aβ ratio by YM201636 was not caused by an altered membrane lipid composition (that is, decreased PtdIns(3,5)P_2 levels). During the endosomal maturation, the lumen of the organelle is gradually acidified as it progresses towards lysosomes. To test whether acidification of endosome is critical to Aβ42 production, we tested several different pH upon membrane incubation. Notably, Aβ42/total Aβ ratio was increased along with decreased pH (Fig. 10i). These data suggest that the degree of acidification in the endosomal compartment, where the γ-secretase resides, is responsible for the increases in Aβ42/total Aβ ratio in the γ-cleavage.